Acta Pharmaceutica Sinica B 2025;15(10):5294−5311

Chinese Pharmaceutical Association
Institute of Materia Medica, Chinese Academy of Medical Sciences

Acta Pharmaceutica Sinica B

www.elsevier.com/locate/apsb
www.sciencedirect.com

ORIGINAL ARTICLE

Succinylation of tumor suppressor PPP2R1A K541 by HAT1 converses the role in modulation of gluconeogenesis/lipogenesis remodeling to display oncogene function

Guang Yang[a,†], Yufei Wang[a,†], Hongfeng Yuan[a,†], Huihui Zhang[a], Lina Zhao[a], Chunyu Hou[a], Pan Lv[a], Jihui Hao[b,*], Xiaodong Zhang[a,*]

[a]*National Key Laboratory of Druggability Evaluation and Systematic Translational Medicine, Department of Gastrointestinal Cancer Biology, Tianjin Cancer Institute, Liver Cancer Center, Tianjin Medical University Cancer Institute and Hospital, National Clinical Research Center for Cancer, Tianjin Key Laboratory of Digestive Cancer, Tianjin 300060, China*
[b]*National Key Laboratory of Druggability Evaluation and Systematic Translational Medicine, Key Laboratory of Cancer Prevention and Therapy, National Clinical Research Center for Cancer, Tianjin Key Laboratory of Digestive Cancer, Tianjin's Clinical Research Center for Cancer, Department of Pancreatic Cancer, Tianjin Medical University Cancer Institute and Hospital, Tianjin 300060, China*

Received 5 June 2024; received in revised form 26 January 2025; accepted 11 March 2025

KEY WORDS

HAT1;
PPP2R1A;
Succinylation;
PCK1 phosphorylation;
Metabolic remodeling;
SREBP1;
Gluconeogenesis;
Lipogenesis;
Liver cancer

Abstract Metabolic reprogramming plays a central role in tumors. However, the key drivers modulating reprogramming of gluconeogenesis/lipogenesis are poorly understood. Here, we try to identify the mechanism by which histone acetyltransferase 1 (HAT1) confers reprogramming of gluconeogenesis/lipogenesis in liver cancer. Diethylnitrosamine (DEN)/carbon tetrachloride (CCl_4)-induced hepatocarcinogenesis was hardly observed in HAT1-knockout mice. Multi-omics identified that HAT1 modulated gluconeogenesis and lipogenesis in liver. Protein phosphatase 2 scaffold subunit alpha (PPP2R1A) promoted gluconeogenesis and inhibited lipogenesis by phosphoenolpyruvate carboxykinase 1 (PCK1) serine 90 dephosphorylation to suppress the tumor growth. HAT1 succinylated PPP2R1A at lysine 541 (K541) to block the assembly of protein phosphatase 2A (PP2A) holoenzyme and interaction with PCK1, resulting in the depression of dephosphorylation of PCK1. HAT1-succinylated PPP2R1A contributed to the remodeling of gluconeogenesis/lipogenesis by PCK1 serine 90 phosphorylation,

*Corresponding authors.
E-mail addresses: zhangxiaodong@tjmuch.com (Xiaodong Zhang), haojihui@tjmuch.com (Jihui Hao).
[†]These authors made equal contributions to this work.
Peer review under the responsibility of Chinese Pharmaceutical Association and Institute of Materia Medica, Chinese Academy of Medical Sciences.

https://doi.org/10.1016/j.apsb.2025.07.040

leading to the inhibition of gluconeogenic enzyme activity and activating sterol regulatory element-binding protein 1 (SREBP1) nuclear accumulation-induced lipogenesis gene expression, which enhanced the tumor growth. In conclusion, succinylation of PPP2R1A lysine 541 by HAT1 converses the role in modulation of gluconeogenesis/lipogenesis remodeling through PCK1 S90 phosphorylation to support liver cancer. Our finding provides new insights into the mechanism by which post-translational modifications (PTMs) confer the conversion of tumor suppressor function to oncogene.

1. Introduction

Metabolic remodeling is a metabolic pattern change during tumorigenesis[1]. Liver cancer is one of the most prevalent and lethal human cancers[2-4]. Increasing evidence indicates that liver cancer is a kind of metabolic disease, and metabolic remodeling plays a critical role in hepatocarcinogenesis and liver cancer progression[5]. A well-recognized emphasis is that aberrant expression and modification of metabolic enzymes in liver cancer cells compared with normal hepatocytes is required for metabolic remodeling during tumorigenesis and tumor growth[6]. Deregulation of carbohydrate metabolism, such as glycolysis, pentose phosphate pathway, and tricarboxylic acid cycle (TCA cycle), has been well-recognized in liver cancer[7]. The significant pro-tumorigenic effect of glycolysis is widely investigated, and gluconeogenesis is a reverse process of glycolysis, generating glucose from small carbohydrate substrates[8]. Accordingly, gluconeogenesis signaling is repressed and gluconeogenesis enzymes are downregulated in cancers[9]. Liver is the main organ for gluconeogenesis, and therefore gluconeogenesis remodeling plays a unique role in liver cancer[10].

Phosphoenolpyruvate carboxykinase 1 (PCK1) is the rate-limiting enzyme in gluconeogenesis and the downregulation of PCK1 is associated with an unfavorable prognosis of liver cancer patients[11]. Meanwhile, tumor cells induce lipogenesis for their unlimited proliferation, in which activating lipogenesis-related transcription factors sterol regulatory element-binding proteins (SREBPs) play a central role[12]. Excitingly, a recent study reports that the phosphorylation of PCK1 at serine 90 (pS90), which is upregulated in liver cancer, promotes the nuclear accumulation of sterol regulatory element-binding protein 1 (SREBP1) and activates the transcription of downstream lipogenesis-related genes, inducing tumor cell proliferation[13]. This important discovery provides an essential possibility of the linkage and coordination between gluconeogenesis and lipogenesis[14]. However, the key factors conferring the remodeling of gluconeogenesis/lipogenesis in liver cancer are poorly understood.

Up to now, post-translational modifications (PTMs) conversing tumor suppressor function to oncogene have not been reported. Protein PTMs, such as phosphorylation and acetylation, are complex and fine-tune cellular mechanisms widely affecting key factors in various critical biological processes of tumorigenesis[15,16]. Lysine succinylation (Ksucc), an evolutionarily conserved PTM like lysine acetylation, has been identified and investigated in recent years, presenting crucial and widespread roles in cancer progression, especially during metabolism regulations[17,18]. Histone acetyltransferase 1 (HAT1) is a type B histone acetyltransferase, and recent studies have demonstrated a variety of new PTM functions in cancers, attracting the investigation for improving the understanding of this classical regulator[19,20]. In addition to acetylation, HAT1 is able to regulate lysine isobutyrylation and methacrylation[21,22]. Our group reports that HAT1 is a new succinyltransferase for the succinylation of phosphoglyceromutase 1 (PGAM1) to induce glycolysis in promoting tumor progression[23]. Meanwhile, some other studies have reported the function of HAT1 in the modulation of metabolic remodeling and cancers, such as HAT1 contributing to the glycolysis in lung cancer, and driving gemcitabine resistance of pancreatic cancer by regulating PVT1/EZH2 complex[24]. However, the effect of HAT1 on the remodeling of gluconeogenesis/lipogenesis in liver cancer remains unclear.

Phosphatases-mediated reversible protein phosphorylation functions as a basic mechanism for cellular processes in cancer cells[25]. Protein phosphatase 2A (PP2A) is a protein complex that contains 60 different holoenzymes, which are distinctly assembled by three classes of subunits, including scaffold subunit A, regulatory subunit B, and catalytic subunit C[26]. PP2A is accountable for the serine/threonine dephosphorylation of 50%−70% human proteins and has been identified as a unique tumor suppressor[27]. The A and C subunits of PP2A present significant sequence conservation in eukaryotic organisms[26]. Protein phosphatase 2 scaffold subunit alpha (PPP2R1A) and protein phosphatase 2 catalytic subunit alpha (PPP2CA) are representative members of A and C subunits of PP2A, respectively[28]. PPP2R1A is required for the assembly of the PP2A complex and shows a high mutation rate in cancers[29]. It has been reported that PPP2R1A regulates epithelial-mesenchymal transition by YAP1 phosphorylation in colorectal cancer[30]. PPP2R1A is involved in B-cell acute lymphoblastic leukemia by modulating PI3K/AKT signaling[31]. However, the investigation of PPP2R1A in the modulation of metabolic remodeling is limited. The functions of PPP2R1A in liver cancer have not been reported yet. The role of PPP2R1A in the modulation of remodeling of gluconeogenesis/lipogenesis in tumors is not well documented.

In the present study, we are interested in the role of HAT1 in modulation of remodeling of gluconeogenesis/lipogenesis in liver cancer. Strikingly, we identified that succinylation of PPP2R1A lysine 541 by HAT1 converts the role in modulation of gluconeogenesis/lipogenesis remodeling through PCK1 S90 phosphorylation to support liver cancer. Thus, the succinylation of tumor suppressor PPP2R1A displays an oncogene function. Our finding provides new insights into the mechanism by which PTMs confer the conversion of tumor suppressor function to oncogene.

2. Materials and methods

2.1. Cell lines and cell culture

Hepatoma cell lines such as HepG2, Huh7, human normal liver cell line LO2, the human kidney epithelial (HEK) 293T cell line

and other types of cancer cell lines such as HuCCT1, PANC1, MCF-7, KYSE180, HCT116, SGC7901, H1299, A498, Hela were obtained from ATCC and BFB, which were cultured in Dulbecco's modified Eagle's medium (DMEM; Gibco, Grand Island, NY, USA) containing 10% fetal bovine serum (FBS, Gibco, Grand Island, NY, USA). All cell lines were treated with 100 U/mL penicillin, and 100 mg/mL streptomycin in a humidified incubator equilibrated with 5% CO_2 at 37 °C. For the function of HAT1 on gluconeogenesis, the cells were cultured under both glucose-starved condition (0.1 mmol/L) and high glucose condition (25 mmol/L). Primary human hepatocytes (PHH) were purchased from RIDL (Shanghai, China) and maintained in William's E medium (Gibco-Invitrogen, Carlsbad, CA, USA) with 5% FCS, 7×10^{-5} mol/L hydrocortisone hemisuccinate, 5 μg/mL insulin and 2% DMSO (Sigma-Cell Culture reagent). Histone acetyltransferase 1 (HAT1) inhibitor JG-2016 was purchased from MCE (Shanghai, China).

2.2. *Plasmid construction and siRNAs*

All plasmids used in this study were constructed by GenScript Biotechnology Co., Ltd. (Nanjing, China) unless specifically stated otherwise, and were listed in Supporting Information Table S1. All primers are listed in Supporting Information Table S2. All siRNAs were synthesized by Sangon Biotech (Shanghai, China). All siRNA sequences are listed in Supporting Information Table S3.

2.3. *MicroPET/CT imaging of mice*

MicroPET/CT imaging of mice was performed using an Inveon MicroPET/CT (Siemens Medical Solution). Briefly, tumor-bearing mice were injected with 11.1 MBq (300 mCi) of 18F-FDG *via* the tail vein. Scanning began 45 min after injection, mice were subjected to a 10-min microCT scan and then to a 10-min microPET scan. Images of mice were reconstructed using a three-dimensional ordered subset expectation maximization (OSEM3D)/maximum algorithm. The Inveon Research Workplace was used to calculate the percentage injected dose per gram (%ID/g) and the SUVs as previously described. The SUVmax was then calculated.

2.4. *RNA extraction and reverse transcription−quantitative PCR (RT−qPCR) analysis*

Total RNAs were extracted from cells using TRIzol reagent (Invitrogen, Carlsbad, CA, USA). RT-qPCR was performed by a Bio-Rad sequence detection system according to the manufacturer's instructions using double-stranded DNA-specific SYBR GreenPremix Ex TaqTM II Kit (TaKaRa, Ohtsu, Japan). Experiments were conducted in duplicate in three independent assays. Relative transcriptional folds were calculated as $2^{-\Delta\Delta Ct}$. GAPDH was used as an internal control for normalization. All the primers used are listed in Table S2.

2.5. *Western blot analysis*

Total protein was isolated from cell lines or tissues by lysis with RIPA buffer. Proteins were subjected to SDS-PAGE and then transferred to a PVDF membrane, blocked with 5% non-fat milk, and incubated with first antibodies for 1 h at room temperature or 12 h at 4 °C. After incubation with secondary antibody against mouse or rabbit for 1 h at 37 °C, the membrane was visualized with an ECL Western Blotting Detection Kit from GE Healthcare (Waukesha, WI, USA). To analyze the nuclear and cytoplasmic levels of sterol regulatory element-binding protein 1 (SREBP1), the proteins from nuclear and cytoplasm of the cells were extracted by using Nuclear and Cytoplasmic Protein Extraction Kit (Beyotime, Shanghai, China) according to the manufacturer's instructions. Histone H3 and β-actin were used as nuclear and cytoplasmic markers, respectively. All antibodies used are documented in Supporting Information Table S4.

2.6. *Immunofluorescence staining and confocal assays*

The expression or colocalization of target proteins was assessed by immunofluorescence staining and confocal assays. Cells cultured on slides in 24-well plates were washed three times with precooled PBS, fixed with 4% paraformaldehyde for 20 min, and permeabilized with 0.5% Triton X-100 at room temperature for 10 min. After incubating for 1 h with 3% BSA, the slides were incubated with the primary antibodies overnight at 4 °C and secondary antibodies for 1 h at room temperature. Images were acquired by using a Nikon A1-R confocal microscope. The antibodies used are listed in Table S4.

2.7. *Nile red staining*

After washing with 1 × PBS, the cultured cells were fixed by 4% paraformaldehyde, and followed by staining with Nile Red solution (7385-67-3, Solarbio, Beijing, China) diluted 1:100 with PBS for 20 min in the dark. Samples were then washed twice with PBS, and stained with DAPI. a Nikon A1-R microscope was used to obtain the images.

2.8. *Coimmunoprecipitation (co-IP) assays*

The CO-IP protocol was described in detail in previously published articles[32]. The cell lysates were harvested and then subjected to overnight immunoprecipitation at 4 °C using 2−5 μg of antibodies listed in Table S4. Immune complexes were incubated with protein A/G agarose beads (Sigma−Aldrich, St. Louis, MO, USA) at 4 °C. The precipitates were washed six times with ice-cold lysis buffer and then resuspended in the PBS. The IP products were resolved by SDS-PAGE followed by Western blot analysis.

2.9. *Hematoxylin and eosin (H&E) staining and immunohistochemistry*

For histological analysis, tumors isolated from liver lobe were fixed in 10% buffered formalin (Fisher HealthCare, 23-245685) for 24 h. Five μm thick sections produced from tumor tissues were prepared and stained with hematoxylin (Sigma−Aldrich, St. Louis, MO, USA) and eosin Y (Thermo Scientific, 6766007). All images were acquired with Nikon Eclipse 80i microscope and EVOS Auto FL2. For immunohistochemistry staining, all microarrays were obtained from Tianjin Medical University Cancer Institute and Hospital (Tianjin, China). Approval for the study protocol was granted by the Research Ethics Committee at Tianjin Medical University Cancer Institute and Hospital (EK2023016). Written consents were acquired from every patient. The tissue microarray information is shown in Supporting Information Table S5. Tumor tissues from nude mice and C57BL/6 mice were fixed and embedded in paraffin after the mice were

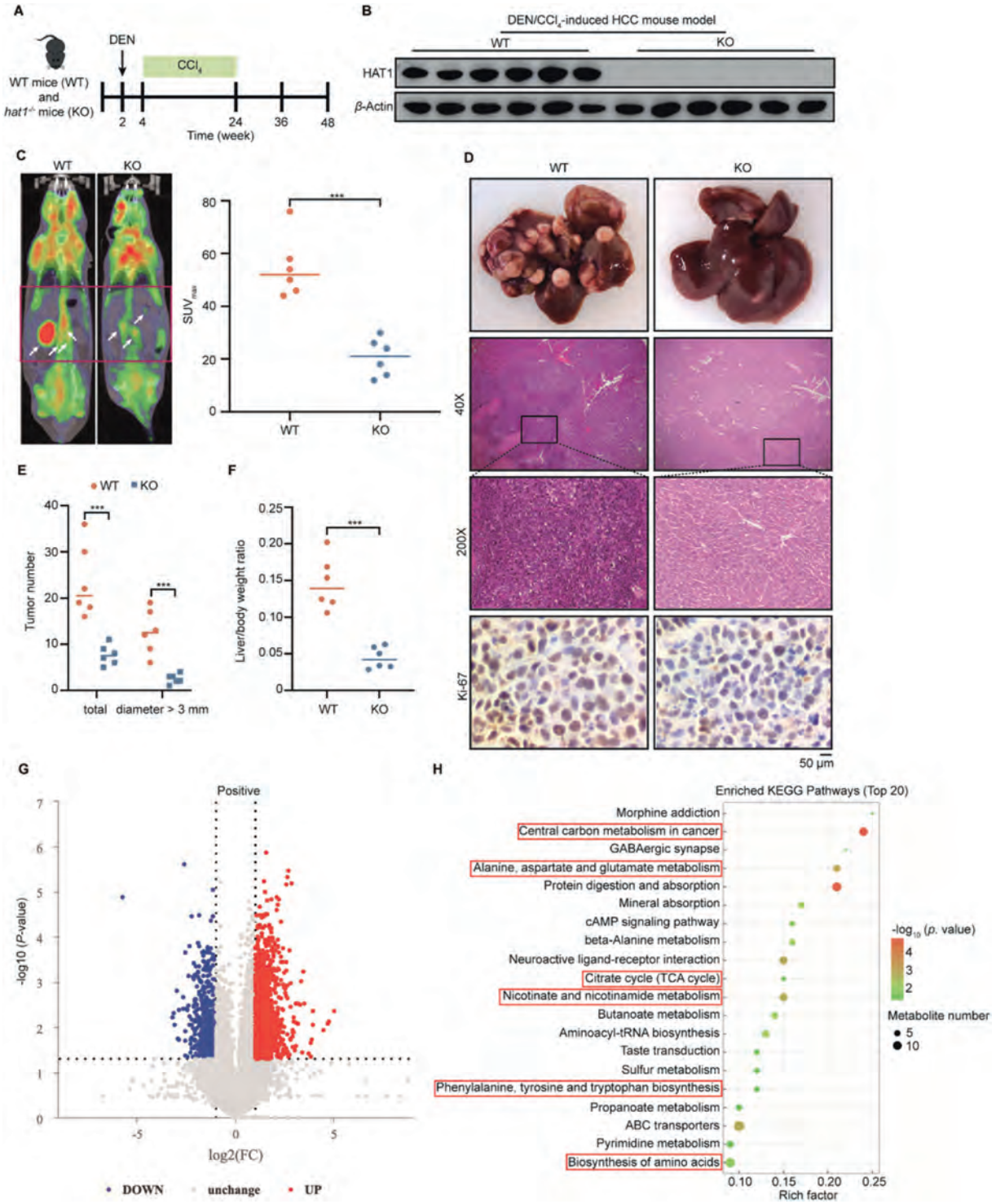

Figure 1 HAT1 is essential for DEN/CCl_4-induced hepatocarcinogenesis. (A) The scheme depicting the experimental outline of the DEN/CCl_4-induced HCC mouse model was shown. The wild type (WT) and liver-specific Hat1 knockout C57BL/6 mice ($Hat1^{-/-}$) mice were administered DEN (25 mg/kg) by i.p. injection on Day 14 after birth and then were administered CCl_4 (0.5 mL/kg) by intraperitoneal injection for 20 weeks after administration of DEN. The mice were analyzed at 48 weeks. (B) The expression of HAT1 was examined by Western blot analysis in liver tissues of WT ($n = 6$) and $Hat1^{-/-}$ mice ($n = 6$) from DEN/CCl_4-induced HCC model. (C) Representative PET/CT images of WT and $Hat1^{-/-}$ mice from the DEN/CCl_4-induced HCC mouse model were shown, and the SUV_{max} values were analyzed in the mice. (D) Representative livers from WT and $Hat1^{-/-}$ mice of DEN/CCl4-induced HCC model were shown. H&E staining and IHC staining of HAT1 and Ki-67 were determined in liver tissues from the mice. Scale bar, 50 μm. (E) The total tumor number and the tumor number (>3 mm) were calculated in the liver of WT ($n = 6$) and $Hat1^{-/-}$ mice from the DEN/CCl_4-induced HCC model ($n = 6$). Each point is one mouse. (F) The liver/body weight ratio was tested in WT and $Hat1^{-/-}$ mice from the DEN/CCl_4-induced HCC model. (G, H) Untargeted metabolomics were performed in liver tissues from WT and

sacrificed. Immunohistochemical analysis was performed as described previously[33]. The primary antibodies were listed in Table S4.

2.10. CCK-8 assays

Hepatoma cells were seeded into 96-well plates (2000 cells/well) for 12 h before transfection. CCK-8 (YEASEN, Shanghai, China) assays were used to assess the cell proliferation every 24 h from the first day until 72 h after transfection.

2.11. Establishment of stable depletion cell lines

HAT1 and phosphoenolpyruvate carboxykinase 1 (PCK1) knockout HepG2 cell lines were established by using CRISPR/Cas9 system previously[23]. Briefly, multiple sgRNAs for HAT1 and PCK1 DNA target were screened from the BlueHeron (https://benchling.com). The sgRNAs were designed based on the target site sequence (21 bp) and needed to be flanked on the 3′ end by a 3 bp NGG PAM sequence. DNA oligonucleotides, which harbored variable 21-nt sequences for Cas9 targeting, were annealed to generate short double-strand DNA and inserted into BbsI-digested plasmid pX330. Three shRNAs targeting HAT1 were designed, among which shHAT1-3 showed the strongest knockdown efficiency in 293T cells and was used in the following experiments.

2.12. Expression and purification of recombinant proteins

The protocol of expression and purification of recombinant proteins was performed as previously described[23]. The CDS region of HAT1 and HAT1 T188A (T to A) were synthesized and constructed into the plasmid of pET-30a (+) by Genscript (Nanjing, China). And then, the plasmids were expressed in BL21 strain of *Escherichia coli*. The cultures grew at 37 °C to an optical density (at a wavelength of 600 nm) of about 0.6 and were then treated with 0.5 mmol/L isopropyl β-D-1-thiogalactopyranoside (IPTG) at 18 °C. Cell pellets were collected, resuspended in BugBuster lysis buffer (EMD Millipore) with a supplement of cocktail proteinase inhibitors and DNase I, and processed using sonication. Soluble His-tagged proteins were purified as described previously[34].

2.13. In vitro succinylation assays

The protocol of expression and purification of recombinant proteins was conducted as previously described[35]. To analyze HAT1-catalyzed PPP2R1A succinylation, we incubated purified wild-type PPP2R1A with purified full-length active HAT1 in the presence of succinylation buffer (50 mmol/L Tris−HCl, pH 8.0, 50 mmol/L KCl, 5% glycerol, 0.1 mmol/L EDTA, 1 mmol/L dithiothreitol, 1 mmol/L PMSF, 10 mmol/L sodiumbutyrate), and 2 μmol/L succinyl-CoA (Sigma, USA), or CoA (Sigma, USA), at 37 °C for 10 min. To analyze the priority of HAT1-catalyzed protein phosphatase 2 scaffold subunit alpha (PPP2R1A) succinylation and acetylation, we incubated purified wild-type PPP2R1A with purified full-length active HAT1 in the presence of succinylation buffer (50 mmol/L Tris−HCl, pH 8.0, 50 mmol/L KCl, 5% glycerol, 0.1 mmol/L EDTA, 1 mmol/L dithiothreitol, 1 mmol/L PMSF, 10 mmol/L sodiumbutyrate), and 2 μmol/L succinyl-CoA and acetyl-CoA (SIGMA, USA), at 37 °C for 10 min.

2.14. Activity assays for PCK1 enzymes and analyses of metabolites

The activity of PCK1 was determined by using the phosphoenolpyruvate carboxykinase activity assay kit (K359, BioVision, CA, USA). In this assay, Phosphoenolpyruvate Carboxykinase was coupled with a set of enzymes that convert PEP and carbonate into a series of intermediates and hydrogen peroxide, which in turn, reacted with a probe and converted generating a colorimetric signal (OD: 570 nm). The cholesterol and triglyceride levels in cells and tumor tissues from nude mice were measured by Cholesterol Assay Kit and Triglyceride Assay Kit (Shanghai Kehua Bioengineering, Shanghai, China) according to the manufacturer's instructions. The PEP and citrate levels in cells and tumor tissues from nude mice were measured by phosphoenolpyruvate (PEP) Colorimetric/Fluorometric Assay Kit (MAK102, Sigma−Aldrich, MO, USA) and Citrate Assay Kit (MAK057, Sigma−Aldrich, MO, USA) according to the manufacturer's instructions.

2.15. Flow cytometry for apoptotic cells analysis

The cell apoptosis was analyzed by a PE Annexin V Apoptosis Detection Kit I (BD, USA). The treated cells were washed with PBS, trypsinized and suspended in PBS. Cells were fixed with cold methanol overnight and suspended in PBS with 20 μg/mL RNase for 30 min at 37 °C, stained with 2 μg/mL propidium iodide for 10 min and analyzed for DNA content by flow cytometry.

2.16. Molecular docking analysis

The docking analysis of PPP2R1A with PCK1 and HAT1 was tested by Discovery Studio software according to the reported methods, with some modifications[36,37]. The docking of PPP2R1A with PCK1 and HAT1 was analyzed by CDOCKER.

2.17. Analysis of tumorigenicity in nude mice

The protocol of analysis of tumorigenicity in nude mice was performed as previously described[23]. HepG2 cells (5×10^6) with or without modified gene expression were subcutaneously injected into male 4-week-old athymic nude mice. For the function of PPP2R1A on the growth of liver cancer cells, thirty mice were randomly grouped into five groups (six per group) before tumor cell injection. Tumor growth was measured after 10 days from injection every 5 days. Tumor volume (V) was monitored by measuring the length (L) and width (W) with calipers and calculated with the formula $\times 0.5$. At 30 days after injection, mice were sacrificed, and the tumor tissues were obtained for further study. For the function of HAT1/PPP2R1A/PCK1 on the growth of liver

Hat1$^{-/-}$ mice of DEN/CCl_4-induced HCC model. (G) Volcano plot depicting the different levels of metabolites (fold change >1.5, or fold change <0.67, $P < 0.05$). (H) Enriched Kyoto Encyclopaedia of Genes and Genomes (KEGG) pathways of differently expressed metabolites were presented. Data are presented as mean ± SD. Student's t-test, ***$P < 0.001$. HAT1: histone acetyltransferase 1, DEN: diethylnitrosamine, CCl_4: carbon tetrachloride, HCC: hepatocellular carcinoma, WT: wild type, H&E: hematoxylin and eosin (H&E), IHC: immunohistochemistry, KEGG: Kyoto Encyclopaedia of Genes and Genomes.

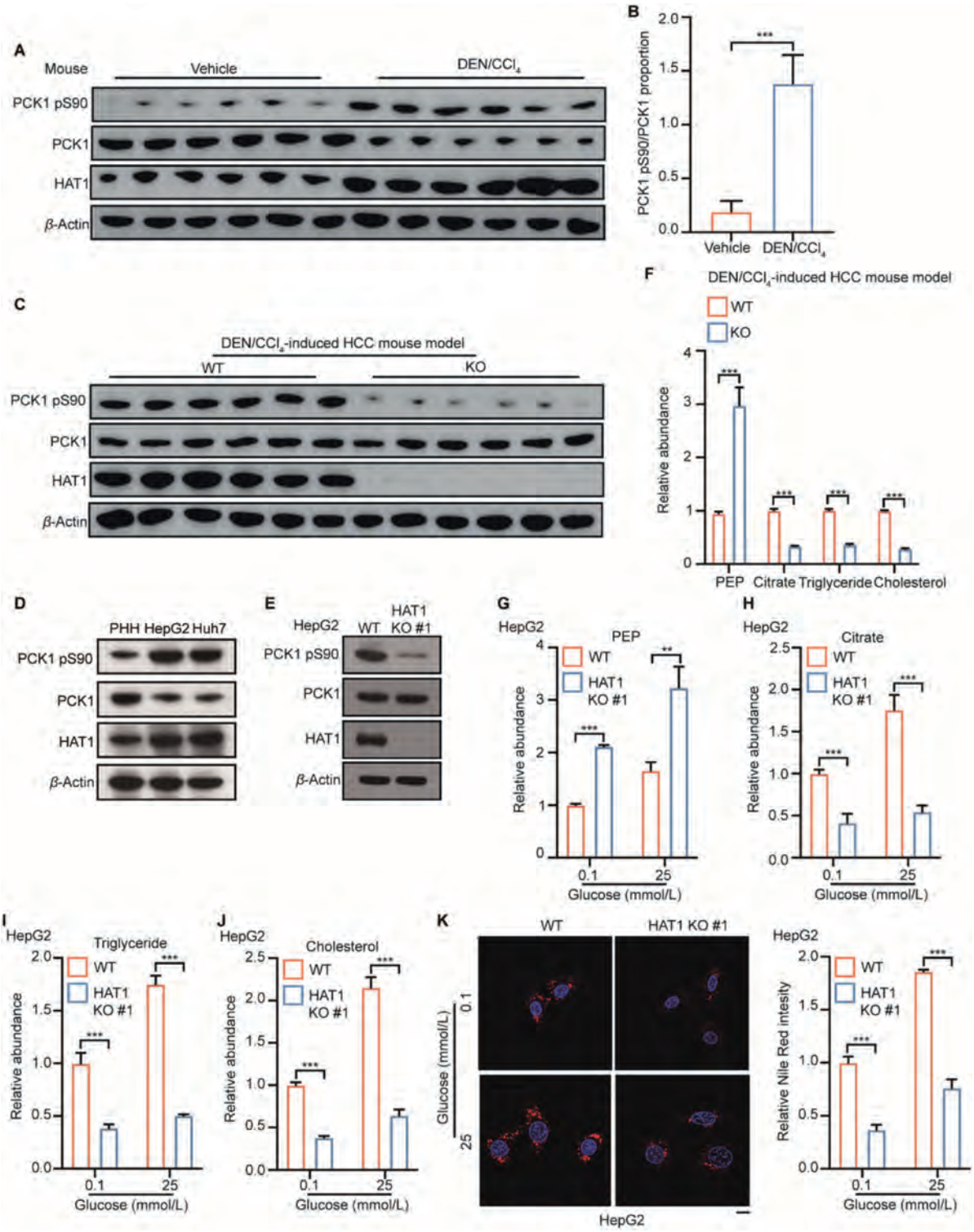

Figure 2 HAT1 confers the remodeling of gluconeogenesis/lipogenesis. (A) A model of HAT1 conferring PCK1-mediated remodeling of gluconeogenesis/lipogenesis. (B) The levels of PCK1 pS90, PCK1, HAT1, and β-actin were detected by Western blot analysis in the liver tissues from C57BL/6 mice treated with normal vehicle ($n = 6$) or C57BL/6 mice of DEN/CCl_4-induced HCC model ($n = 6$). (C) The levels of PCK1 pS90, PCK1, HAT1, and β-actin were measured by Western blot analysis in liver tissues of WT ($n = 6$) and *Hat1*$^{-/-}$ mice ($n = 6$) from DEN/CCl_4-induced HCC model. (D) The levels of PCK1 pS90, PCK1, HAT1, and β-actin were determined by Western blot analysis in primary human hepatocytes (PHH), HepG2, and Huh7 cells. (E) The levels of PCK1 pS90, PCK1, HAT1, and β-actin were examined by Western blot analysis in WT HepG2 cells and HAT1 KO Clone 1 HepG2 cells (HAT1 KO #1). (F) The relative levels of PEP, citrate, triglyceride, and cholesterol were analyzed by the corresponding assay kits in the liver tissues of WT ($n = 6$) and *Hat1*$^{-/-}$ mice ($n = 6$) from DEN/CCl_4-induced HCC model, respectively. (G–J) The relative levels of PEP, citrate, triglyceride, and cholesterol were tested by the corresponding assay kits in WT HepG2 cells

cancer cells, forty-eight mice were randomly grouped in eight groups (six per group) before tumor cell injection. Tumor growth was measured after 10 days from injection every 5 days. Tumor volume (V) was monitored by measuring the length (L) and width (W) with calipers and calculated with the formula $\times$ 0.5. At 30 days after injection, mice were sacrificed, and the tumor tissues were obtained for further study. The apoptosis was analyzed by TUNEL staining in the tumor tissues (Abcam, ab206386, USA). The Institute Research Ethics Committee at Tianjin Medical University Cancer Institute and Hospital approved the study protocol (NSFC-AE-2023028).

2.18. Mice and DEN/CCl_4 model

Hat1 floxed mice ($Hat1^{fl/fl}$) were bred with albumin-Cre mice to establish hepatocyte-specific *Hat1* knockout (KO) C57BL/6N ($Hat1^{fl/fl;Alb\text{-}Cre}$) mice (Cyagen Biosciences, Suzhou, China), as previously described by us[38]. The genotyping was performed by standard PCR protocols. For diethylnitrosamine (DEN) model, 25 mg/kg of DEN (Sigma−Aldrich, St. Louis, MO, USA) was administered i.p. into 14-day-old male mice. The mice were then administered carbon tetrachloride (CCl_4) (0.5 mL/kg) by intraperitoneal injection for 20 weeks after administration of DEN. Mice were maintained on autoclaved water and regular chow diet and analyzed at 48 weeks. All animal experiments were approved by Institute Research Ethics Committee at Tianjin Medical University Cancer Institute and Hospital (NSFC-AE-2023028).

2.19. Statistical analysis

Each experiment was repeated at least three times. Statistical significance was assessed by comparing mean values ($\pm$ standard deviation, SD) using a Student's t-test for independent groups and was assumed for $^*P < 0.05$; $^{**}P < 0.01$; $^{***}P < 0.001$ unless specifically indicated.

3. Results

3.1. HAT1 is essential for DEN/CCl_4-induced hepatocarcinogenesis

HAT1 is a key factor with multiple modification functions in tumors[20]. We established liver-specific *Hat1* knockout mice ($Hat1^{-/-}$ mice) and validated the expression of HAT1 in the tissues of liver, heart, spleen, lung and kidney from the wild type mice (WT mice) and $Hat1^{-/-}$ mice, and failed to observe the expression of HAT1 in liver of knockout mice (Supporting Information Fig. S1A). To determine the effect of HAT1 on hepatocarcinogenesis, we established a DEN/CCl_4-induced liver cancer mouse model using WT mice and $Hat1^{-/-}$ mice (Fig. 1A). The knockout of *HAT1* was validated in the liver tissues from $Hat1^{-/-}$ mice (Fig. 1B). Interestingly, the MicroPET/CT system revealed that $Hat1^{-/-}$ mice exhibited obviously lower SUV_{max} relative to that of WT mice after 24 weeks of DEN/CCl_4 treatment (Fig. 1C). After the anatomy, $Hat1^{-/-}$ mice showed few liver cancer incidences, reduced tumor burden, smaller histological lesions, and inhibited Ki-67 levels compared with the WT counterparts (Fig. 1D and Fig. S1B), suggesting that the knockout of HAT1 significantly restrains the development of liver cancer. Consistently, total tumor number, the tumor number (diameter $>$3 mm), and liver/body weight ratio were significantly suppressed in $Hat1^{-/-}$ mice (Fig. 1E and F). To further clarify the biological function of HAT1 in hepatocarcinogenesis, we performed a multi-omics, including RNA-sequencing, phosphoproteomics, and untargeted metabolomics, in liver tissues of WT and $Hat1^{-/-}$ mice (Supporting Information Fig. S2A). Interestingly, we identified 384 upregulated and 801 downregulated differentially expressed genes (DEGs) in liver tissues of $Hat1^{-/-}$ mice compared with those of WT mice (Fig. S2B). Kyoto Encyclopedia of Genes and Genomes (KEGG) pathway analysis of DEGs revealed that the depletion of HAT1 significantly affected several crucial signaling pathways, such as TNF signaling pathway, TGF-β signaling pathway, and Hippo signaling pathway (Fig. S2C). Importantly, phosphoproteomics identified 46 upregulated and 202 downregulated phosphopeptides in liver tissues of $Hat1^{-/-}$ mice relative to those of WT mice (Fig. S2D). Intriguingly, KEGG pathway analysis of different phosphoproteins showed an obvious effect of HAT1 on phosphorylation signaling in the liver, including AMPK signaling pathway, cGMP−PKG signaling pathway, and glycolysis/gluconeogenesis signaling pathway (Fig. S2E). For untargeted metabolomics, 124 differential metabolites were displayed in the liver tissues of $Hat1^{-/-}$ mice compared with those of WT mice (Fig. S2F). Importantly, our data identified the significantly enriched metabolites related to gluconeogenesis or lipogenesis affected by HAT1 depletion in liver (Fig. S2G and S2H). Consistently, untargeted metabolomics in liver tissues from WT and $Hat1^{-/-}$ mice of DEN/CCl_4-induced liver cancer model identified 322 differential metabolites, which were significantly enriched in gluconeogenesis or lipogenesis (Fig. 1G and H, Supporting Information Fig. S3), suggesting that HAT1 may contribute to the hepatocarcinogenesis by affecting gluconeogenesis and lipogenesis processes. Thus, we conclude that HAT1 is essential for DEN/CCl_4-induced hepatocarcinogenesis, conferring gluconeogenesis and lipogenesis processes.

3.2. HAT1 confers the remodeling of gluconeogenesis/lipogenesis

Gluconeogenesis and lipogenesis are two fundamental metabolic processes in liver cancer[9,10]. Gluconeogenic enzyme PCK1 phosphorylation at serine 90 (pS90) activates lipogenesis in hepatocellular carcinoma[13]. Our phosphoproteomics in WT and $Hat1^{-/-}$ mice identified that HAT1 was able to affect phosphorylation of PCK1 in liver and we wondered whether HAT1 was involved in the PCK1-mediated remodeling of gluconeogenesis/lipogenesis in hepatocarcinogenesis. We validated that the pS90 levels of PCK1, but not PCK1 expression, were reduced in liver tissues of $Hat1^{-/-}$ mice ($n = 6$) compared to that of WT mice (Supporting Information Fig. S4A). Intriguingly, the levels of HAT1 and PCK1 pS90 were elevated but PCK1 expression was

and HAT1 KO #1 HepG2 cells cultured in 25 or 0.1 mmol/L glucose conditions for 10 h, respectively. (K) The lipid accumulation was analyzed by Nile Red staining in WT HepG2 cells and HAT1 KO #1 HepG2 cells cultured in 25 or 0.1 mmol/L glucose conditions for 10 h, respectively. Scale bar, 5 μm. The relative Nile Red staining intensity was quantified. Data are presented as mean $\pm$ SD. Student's t-test, $^{**}P < 0.01$, $^{***}P < 0.001$. HAT1: histone acetyltransferase 1, PCK1: phosphoenolpyruvate carboxykinase 1, pS90: phosphorylation at serine 90, DEN: diethylnitrosamine, CCl_4: carbon tetrachloride, HCC: hepatocellular carcinoma, WT: wild type, KO: knockout, PEP: phosphoenolpyruvate.

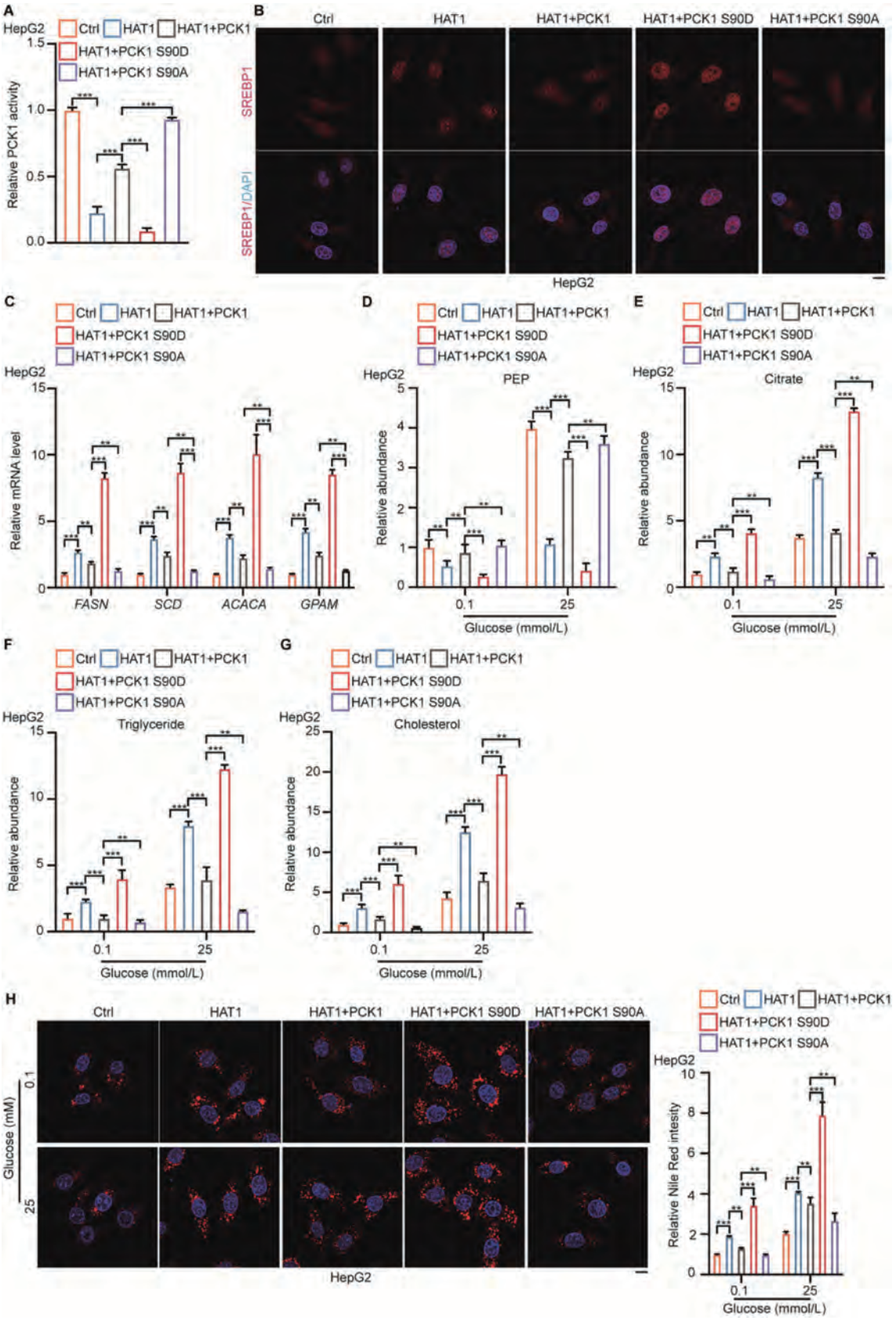

Figure 3 HAT1 triggers the remodeling of gluconeogenesis/lipogenesis by modulating the levels of phosphorylation of PCK1 Ser90. (A−H) HepG2 cells were transfected with plasmids overexpressing HAT1, or co-transfected with plasmids overexpressing HAT1 and PCK1, PCK1 mutant (S90D), or PCK1 mutant (S90A), respectively. (A) The relative PCK1 activity was analyzed by the corresponding assay kit in the cells. (B) The nuclear accumulation of SREBP1 was observed by confocal immunofluorescence analysis in the cells. Scale bar, 5 μm. (C) The mRNA

reduced in liver tissues from DEN/CCl_4-induced liver cancer mice relative to that from vehicle control mice (Fig. 2A and B), while the knockout of HAT1 significantly repressed pS90 levels of PCK1, but not PCK1 expression, in liver tissues of DEN/CCl_4-induced liver cancer mice ($n = 6$) (Fig. 2C), suggesting that HAT1 is essential for remodeling of PCK1 pS90 during hepatocarcinogenesis *in vivo*. Consistently, our data revealed that the levels of HAT1 and PCK1 pS90 were increased but PCK1 expression was downregulated in HepG2 and Huh7 liver cancer cells compared to that in primary human hepatocytes (PHH) and immortalized human normal liver LO2 cells (Fig. 2D and Fig. S4B). The depletion of HAT1 remarkably suppressed the PCK1 pS90 levels of PCK1, but not PCK1 expression, in PHH and HepG2 cells (Fig. 2E, Fig. S4C and S4D). Clinically, IHC staining analysis showed that the levels of HAT1 and PCK1 pS90 were elevated in clinical liver cancer tissues ($n = 49$) relative to that from peritumor tissues ($n = 49$) (Fig. S4E and S4F), and the expression of HAT1 was positively correlated with PCK1 pS90 levels in the liver cancer tissues ($n = 49$) (Fig. S4G). Interestingly, we observed that the depletion of HAT1 was able to reduce the levels of PCK1 pS90 in those cancer cell lines, such as liver cancer HepG2 cells, cholangiocarcinoma HuCCT1 cells, pancreatic cancer PANC1 cells, and renal cancer A498 cells, but not in breast cancer MCF-7 cells, esophageal squamous cell carcinoma KYSE180 cells, colon cancer HCT116 cells, gastric cancer SGC7901 cells, lung cancer H1299 cells, and cervical cancer Hela cells (Fig. S4H), implying that HAT1 may regulate PCK1 pS90 in the cells of cholangiocarcinoma, pancreatic cancer, and renal cancer.

To better understand the effect of HAT1 on gluconeogenesis and lipogenesis during hepatocarcinogenesis, we analyzed the metabolites of gluconeogenesis and lipogenesis in liver. PCK1 catalyzes the conversion of oxaloacetate (OAA) to phosphoenolpyruvate (PEP) in gluconeogenesis and consequently reduces citrate levels of TCA cycle in liver[6]. Triglyceride and cholesterol are two main metabolites in lipogenesis. Our data revealed that the levels of PEP were increased, but citrate, triglyceride, and cholesterol were decreased in the liver tissues of *Hat1*$^{-/-}$ mice relative to those of WT mice in both physiological conditions and DEN/CCl_4-induced liver cancer model (Fig. 2F and Supporting Information Fig. S5A). Intriguingly, the depletion of HAT1 promoted the levels PEP, but inhibited the levels of citrate, triglyceride, cholesterol, and lipid accumulation under both glucose-starved condition (0.1 mmol/L) and high glucose condition (25 mmol/L) in PHH and HepG2 cells (Fig. 2G−K and Fig. S5B−S5I). Thereby, we conclude that HAT1 confers the remodeling from gluconeogenesis to lipogenesis in tumor.

3.3. HAT1 triggers the remodeling of gluconeogenesis/lipogenesis by modulating the levels of phosphorylation of PCK1 Ser90

Mutation of Ser90 in PCK1 to alanine (S90A) blocks PCK1 phosphorylation, and mutation of Ser90 in PCK1 to asparticacid (S90D) mimics PCK1 phosphorylation[13]. The phosphorylation of PCK1 promotes lipogenesis by inducing nuclear accumulation of SREBP1 and transcription of downstream lipogenesis-related genes[13]. Thus, we supposed that HAT1 might trigger the conversion remodeling from gluconeogenesis to lipogenesis by modulating phosphorylation of PCK1 in the cells. We observed that the gluconeogenic enzyme activity of PCK1 was significantly inhibited by overexpression of HAT1 in HepG2 and Huh7 cells, while co-overexpression of PCK1 could rescue that in the cells (Fig. 3A and Supporting Information Fig. S6A). Intriguingly, PCK1 (S90D) remarkably reduced and PCK1 (S90A) enhanced the HAT1-inhibited gluconeogenic enzyme activity of PCK1 in the cells (Fig. 3A and Fig. S6A). Conversely, HAT1 enhanced nuclear accumulation of PCK1 pS90, SREBP1 and expression of SREBP1 target genes associated with lipogenesis, including fatty acid synthase (FASN), stearoyl-CoA desaturase (SCD), acetyl-CoA carboxylase alpha (ACACA), and glycerol-3-phosphate acyltransferase 1 (GPAM), whereas PCK1 attenuated the phenotype in the cells (Fig. 3B and C, and Fig. S6B and S6C). Moreover, S90D mutation of PCK1 promoted and PCK1 mutant (S90A) repressed the HAT1-induced PCK1 pS90, SREBP1 nuclear accumulation and expression of downstream lipogenesis-related genes in the cells (Fig. 3B and C, and Fig. S6B and S6C). Importantly, overexpression of PCK1 reversed HAT1-inhibited PEP levels and HAT1-upregulated levels of citrate, triglyceride, cholesterol, and lipid accumulation under both glucose-starved condition (0.1 mmol/L) and high glucose condition (25 mmol/L) (Fig. 3D−H, and Fig. S6D−S6G). Remarkably, PCK1 (S90D) reinforced and PCK1 (S90A) blocked the effect of HAT1 on gluconeogenesis and lipogenesis phenotypes in the cells (Fig. 3D−H, and Fig. S6D−S6G). Interestingly, PEP levels were increased, and levels of citrate, triglyceride, and cholesterol were decreased by HAT1 knockout and depletion of PCK1 reversed the phenotypes in HepG2 cells (Supporting Information Fig. S7A−S7D). Remarkably, reconstitution of wild-type PCK1, but not PCK1 mutant (S90D), reversed the effect of PCK1 knockdown on the levels of PEP, citrate, triglyceride, and cholesterol (Fig. S7A−S7D). In addition, we constructed PCK1 knockout HepG2 cells, and re-transfected with plasmids overexpressing PCK1, PCK1 mutant (S90D), or PCK1 mutant (S90A) (Supporting Information Fig. S8A). The levels of PEP were decreased and levels of citrate, triglyceride, cholesterol were increased in PCK1 knockout HepG2 cells under both glucose-starved condition (0.1 mmol/L) and high glucose condition (25 mmol/L) (Fig. S8B−S8E). Importantly, overexpression of PCK1 reversed PCK1 knockout-decreased PEP levels and PCK1 knockout-increased levels of citrate, triglyceride, cholesterol, and lipid accumulation under both glucose-starved condition (0.1 mmol/L) and high glucose condition (25 mmol/L) (Fig. S8B−S8E). PCK1 (S90D) reinforced and PCK1 (S90A) blocked the effect of PCK1 knockout on gluconeogenesis and lipogenesis phenotypes in the cells (Fig. S8B−S8E). Taken together, we conclude that HAT1 triggers the remodeling of

expression levels of SREBP1 target genes, including *FASN*, *SCD*, *ACACA*, and *GPAM*, were analyzed by RT-qPCR in the cells. (D−G) The relative levels of PEP, citrate, triglyceride, and cholesterol were measured by the corresponding assay kits in the cells cultured in 25 or 0.1 mmol/L glucose conditions for 10 h, respectively. (H) The lipid accumulation was showed by Nile Red staining in the cells cultured in 25 or 0.1 mmol/L glucose conditions for 10 h, respectively. Scale bar, 5 μm. The relative Nile Red staining intensity was quantified. Data are presented as mean ± SD. Student's *t*-test, $^{**}P < 0.01$, $^{***}P < 0.001$. HAT1: histone acetyltransferase 1, PCK1: phosphoenolpyruvate carboxykinase 1, pS90: phosphorylation at serine 90, SREBP1: sterol regulatory element-binding protein 1, FASN: fatty acid synthase, SCD: stearoyl-CoA desaturase, ACACA: acetyl-CoA carboxylase alpha, GPAM: glycerol-3-phosphate acyltransferase 1.

gluconeogenesis/lipogenesis by modulating the levels of phosphorylation of PCK1 Ser90 in liver cancer.

3.4. HAT1 succinylates PPP2R1A K541, leading to phosphorylation of PCK1 Ser90

Next, we explored the mechanism by which HAT1 regulated phosphorylation of PCK1 Ser90 to drive the remodeling of gluconeogenesis/lipogenesis in liver cancer. A recent study reports that AKT-mediated phosphorylation of PCK1 at serine 90 (pS90) promotes lipogenesis and inhibits gluconeogenesis in tumors[13]. We observed that HAT1 failed to affect expression and phosphorylation of AKT in HepG2 cells (Supporting Information Fig. S9A). Our previous study reports that acetyltransferase HAT1 is a succinyltransferase in tumorigenesis and mutation of threonine 188 at catalytic pocket to alanine (T188A) blocks succinylation enzymatic activity of HAT1[23]. The succinylation of phosphatases scaffold PPP2R1A at lysine 541 (K541) was suppressed by HAT1 knockout in succinylation quantitative proteomics[23]. PP2A is accountable for the serine/threonine dephosphorylation of 50%−70% human proteins[27]. Hence, we wondered whether HAT1 promoted PCK1 pS90 by modulation of PPP2R1A succinylation. The succinylation levels of PPP2R1A were enhanced but the expression of PPP2R1A was reduced in HepG2 cells relative to PHH (Fig. S9B). Importantly, the levels of PPP2R1A succinylation were enhanced but the levels of PPP2R1A expression were reduced in tumor tissues of liver from DEN/CCl_4-induced liver cancer mice relative to those from the liver tissues of vehicle control mice (Fig. 4A), while the knockout of HAT1 significantly repressed PPP2R1A succinylation, but not PPP2R1A expression, in the tumor tissues of DEN/CCl_4-induced liver cancer mice (Fig. 4B), suggesting that HAT1 is responsible for the remodeling of PPP2R1A succinylation during hepatocarcinogenesis *in vivo*. We then validated that the succinylation of PPP2R1A was significantly inhibited by HAT1 knockout in HepG2 cells, and re-expression of wild-type HAT1, but not HAT1 (T188A), could rescue PPP2R1A succinylation in the cells (Fig. 4C and Fig. S9C), suggesting that HAT1 induces PPP2R1A succinylation in liver cancer. Similarly, the levels of PPP2R1A succinylation were reduced by HAT1 inhibitor JG-2016 in HepG2 cells, and re-expression of wild-type HAT1, but not HAT1 (T188A), could rescue the levels of PPP2R1A succinylation in the cells (Fig. S9D). To validate whether HAT1 regulated succinylation of PPP2R1A at K541, we generated an antibody against succinylation of PPP2R1A K541 (PPP2R1A$^{K541\ succ}$). We observed that the levels of PPP2R1A K541 succinylation were reduced by HAT1 knockout or HAT1 inhibitor JG-2016 in HepG2 cells using PPP2R1A$^{K541\ succ}$, and re-expression of wild-type HAT1, but not HAT1 (T188A), could rescue the levels of PPP2R1A K541 succinylation in the cells (Fig. 4D and Fig. S9E). GST pull-down assays indicated that wild-type HAT1 and HAT1 (T188A) were able to directly interact with PPP2R1A, in which the mutant of T188A failed to affect the interaction (Fig. S9F).

In our system, the mutation of lysine (K) to arginine (R) can block the succinylation, and the mutation of lysine (K) to glutamate (E) can mimic the succinylation in cells. We then explore whether HAT1 directly catalyzed the succinylation PPP2R1A. Interestingly, the succinylation of flag-PPP2R1A, but not flag PPP2R1A mutant (K541R), was repressed by HAT1 knockout in HepG2 cells, and re-expression of wild-type HAT1, but not HAT1 (T188A), could rescue the succinylation in the cells (Fig. S9G), suggesting that HAT1 regulates PPP2R1A succinylation at K541 in liver cancer cells. The *in vitro* succinylation assays revealed that HAT1, but not heat-inactivated HAT1, was able to succinylate PPP2R1A, but we failed to observe the HAT1-mediated acetylation of PPP2R1A *in vitro* (Fig. 4E and Fig. S9H). Consistently, CoA could repress HAT1-mediated PPP2R1A succinylation in a dose-dependent manner *in vitro* (Fig. S9I), suggesting that HAT1 can directly catalyze the succinylation of PPP2R1A. Protein phosphatase 2A (PP2A) consists of scaffold subunit PPP2R1A, regulatory subunit PPP2R5E, and catalytic subunit PPP2CA, in which the interaction of scaffold subunit PPP2R1A with catalytic subunit PPP2CA and de-phosphorylated substrates is required for PP2A phosphatase activity[26]. Accordingly, we wondered whether HAT1 contributes to the PCK1 pS90 by affecting the interaction of PPP2R1A with PPP2CA and PCK1 *via* the modulation of PPP2R1A succinylation. Intriguingly, the knockout of HAT1 or HAT1 inhibitor JG-2016 significantly enhanced the interaction of PCK1 with both PPP2R1A and PPP2CA in HepG2 cells, in which re-expression of wild-type HAT1, but not HAT1 (T188A), remarkably destroyed the interaction in the system (Fig. 4F, Fig. S9J and S9K). Furthermore, the depletion of HAT1 or HAT1 inhibitor JG-2016 was able to promote the interaction of PPP2R1A with both PCK1 and PPP2CA in HepG2 cells, and re-expression of wild-type HAT1, but not HAT1 (T188A), suppressed the interaction in the cells (Fig. 4G, Fig. S9L and S9M). However, HAT1 and HAT1 (T188A) failed to affect the interaction of PCK1/PPP2CA with PPP2R1A (K541R), in which the mutation of K541 to R blocked the PPP2R1A succinylation (Fig. 4G, Fig. S9L and S9M), suggesting that HAT1-mediated PPP2R1A succinylation restrains the interaction among PCK1, PPP2R1A, and PPP2CA. Moreover, we analyzed the structure of interaction of PPP2R1A with PCK1 by using the molecular docking analysis, in which aspartic acid 571, valine 584, threonine 583, phenylalanine 577, lysine 541, phenylalanine 537, phenylalanine 502, histidine 453, valine 495, valine 451, leucine 450, valine 454, alanine 456, tryptophan 416, asparagine 534 at PPP2R1A were the critical sites for the interaction (Fig. S9N). In addition, the structure analysis demonstrated the interaction of PPP2R1A with HAT1, and observed that lysine 545, phenylalanine 577, alanine 456, leucine 450, asparagine 505, phenylalanine 501 at PPP2R1A were the critical sites for the interaction (Fig. S9N).

Next, we supposed that HAT1 might block the dephosphorylation of PCK1 Ser90 by succinylation of PPP2R1A to support remodeling of gluconeogenesis/lipogenesis. We observed that the overexpression of HAT1 induced PCK1 pS90, but not PPP2R1A expression, in HepG2 and Huh7 cells, while PPP2R1A, but not PPP2R1A (K541E), could significantly repress HAT1-induced PCK1 pS90 in the cells (Fig. 4H and Supporting Information Fig. S10A). Overexpression of PPP2R1A rescued HAT1-inhibited gluconeogenic enzyme activity of PCK1 in HepG2 and Huh7 cells, while PPP2R1A (K541E) failed to work in the system (Fig. 4I and Fig. S10B). Remarkably, HAT1-induced nuclear accumulation of SREBP1 and expression of SREBP1 target genes, including FASN, SCD, ACACA, and GPAM, were repressed by PPP2R1A, but not PPP2R1A (K541E), in the cells (Fig. 4J and K, Fig. S10C). Consistently, HAT1-reduced PEP levels and HAT1-enhanced levels of citrate, triglyceride, cholesterol, and lipid accumulation were reversed by PPP2R1A under both glucose-starved condition (0.1 mmol/L) and high glucose condition (25 mmol/L), in which PPP2R1A (K541E) mutation destroyed the effect of PPP2R1A on the phenotype (Fig. 4L and M, Fig. S10D). Clinically, IHC staining showed that the levels of nuclear SREBP1 and succinylation of PPP2R1A K541 were

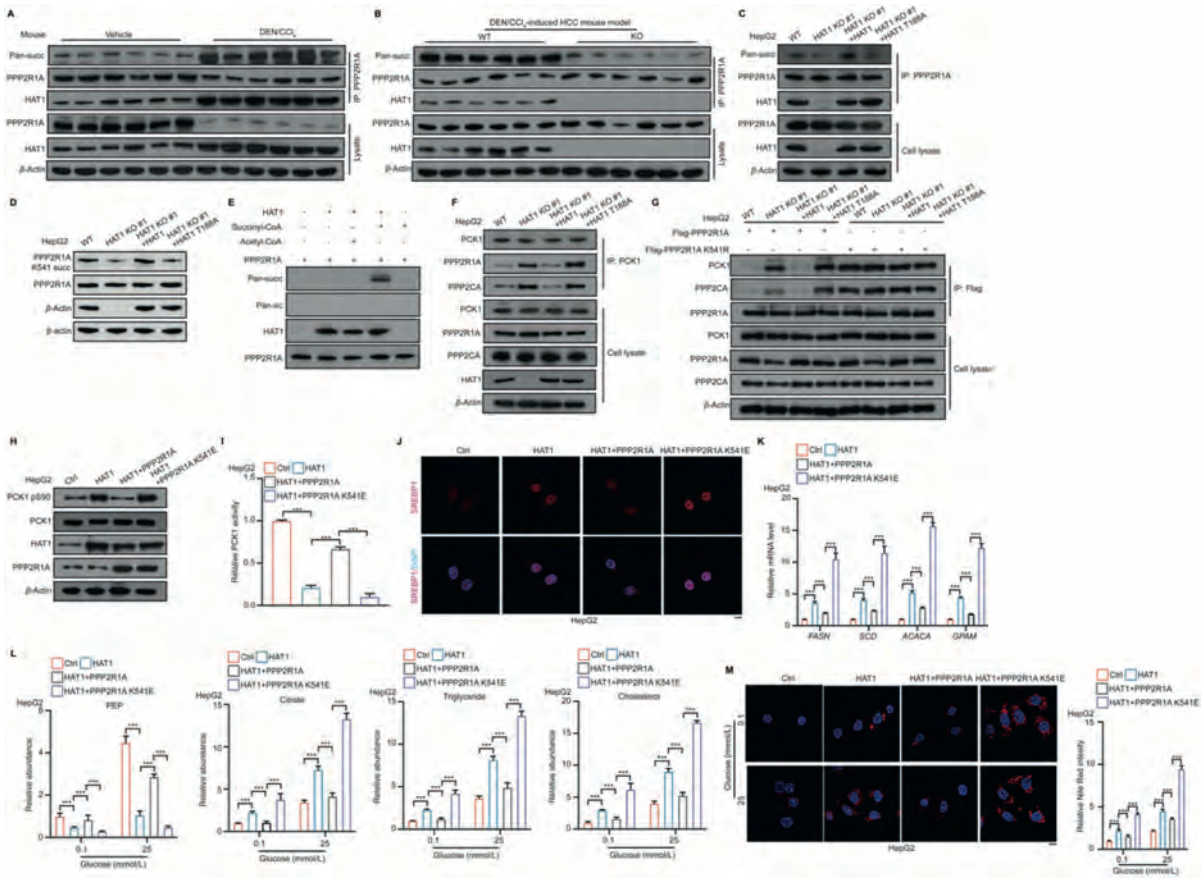

Figure 4 HAT1 succinylates PPP2R1A K541, leading to phosphorylation of PCK1 Ser90. (A) The levels of PPP2R1A succinylation and HAT1 were examined by immunoprecipitation and Western blot analysis as indicated in the liver tissues from C57BL/6 mice treated with normal vehicle ($n = 6$) or tumor tissues from C57BL/6 mice of DEN/CCl_4-induced HCC model ($n = 6$). (B) The levels of PPP2R1A succinylation and HAT1 were measured by immunoprecipitation and Western blot analysis as indicated in tumor tissues of WT ($n = 6$) and *Hat1*$^{-/-}$ mice ($n = 6$) from DEN/CCl_4-induced HCC model, respectively. (C) The PPP2R1A succinylation levels and HAT1 were determined by immunoprecipitation and Western blot analysis as indicated in HepG2 cells (WT), HAT1 KO #1 HepG2 cells, HAT1 KO #1 HepG2 cells reconstituted with wild-type HAT1 or HAT1 mutant (T188A). (D) The levels of PPP2R1A K541 succinylation, PPP2R1A, and HAT1 were measured by Western blot analysis in HepG2 cells (WT), HAT1 KO #1 HepG2 cells, HAT1 KO #1 HepG2 cells reconstituted with wild-type HAT1 or HAT1 mutant (T188A). (E) HAT1-catalyzed PPP2R1A succinylation was analyzed by *in vitro* succinylation assays using purified HAT1, PPP2R1A, and succinyl-CoA/acetyl-CoA as indicated. Western blot analysis was performed using the indicated antibodies. (F) The interaction of PCK1 with PPP2R1A or PPP2CA was analyzed by immunoprecipitation and Western blot analysis as indicated in HepG2 cells (WT), HAT1 KO #1 HepG2 cells, HAT1 KO #1 HepG2 cells reconstituted with wild-type HAT1 or HAT1 mutant (T188A). (G) The interaction of flag-PPP2R1A or flag PPP2R1A mutant (K541R) with PCK1 or PPP2CA was examined by immunoprecipitation and Western blot analysis as indicated in HepG2 cells (WT), HAT1 KO #1 HepG2 cells, HAT1 KO #1 HepG2 cells reconstituted with wild-type HAT1 or HAT1 mutant (T188A). (H−M) HepG2 cells were transfected with plasmids overexpressing HAT1, or co-transfected with plasmids overexpressing HAT1 and PPP2R1A or PPP2R1A mutant (K541E), respectively. (H) The levels of PCK1 pS90, PCK1, HAT1, PPP2R1A, and β-actin were examined by Western blot analysis in the cells. (I) The relative PCK1 activity was detected by the corresponding assay kit in the cells. (J) The nuclear accumulation of SREBP1 was observed by confocal immunofluorescence analysis in the cells. Scale bar, 5 μm. (K) The mRNA expression levels of SREBP1 target genes, including FASN, SCD, ACACA, and GPAM, were analyzed by RT-qPCR in the cells. (L) The relative levels of PEP, citrate, triglyceride, and cholesterol were tested by the corresponding assay kits in the cells cultured in 25 or 0.1 mmol/L glucose conditions for 10 h, respectively. (M) The lipid accumulation was measured by Nile Red staining in the cells cultured in 25 or 0.1 mmol/L glucose conditions for 10 h, respectively. Scale bar, 5 μm. The relative Nile Red staining intensity was quantified. Data are presented as mean ± SD. Student's *t*-test, ***$P < 0.001$. HAT1: histone acetyltransferase 1, PCK1: phosphoenolpyruvate carboxykinase 1, pS90: phosphorylation at serine 90, DEN: diethylnitrosamine, CCl_4: carbon tetrachloride, HCC: hepatocellular carcinoma, WT: wild type, KO: knockout, PPP2R1A: protein phosphatase 2 scaffold subunit alpha, PPP2CA: protein phosphatase 2 catalytic subunit alpha, PEP: phosphoenolpyruvate, SREBP1: sterol regulatory element-binding protein 1, FASN: fatty acid synthase, SCD: stearoyl-CoA desaturase, ACACA: acetyl-CoA carboxylase alpha, GPAM: glycerol-3-phosphate acyltransferase 1.

elevated in the clinical liver cancer tissues ($n = 49$) relative to those in the peritumor tissues ($n = 49$) (Supporting Information Fig. S11A). The levels of PPP2R1A K541 succinylation were positively correlated with those of HAT1, PCK1 pS90 and nuclear SREBP1 in the liver cancer tissues ($n = 49$). The levels of nuclear SREBP1 were positively correlated with those of HAT1 and PCK1 pS90 in the system (Fig. S11B). Meanwhile, the levels of HAT1, PCK1 pS90, nuclear SREBP1, and PPP2R1A K541 succinylation

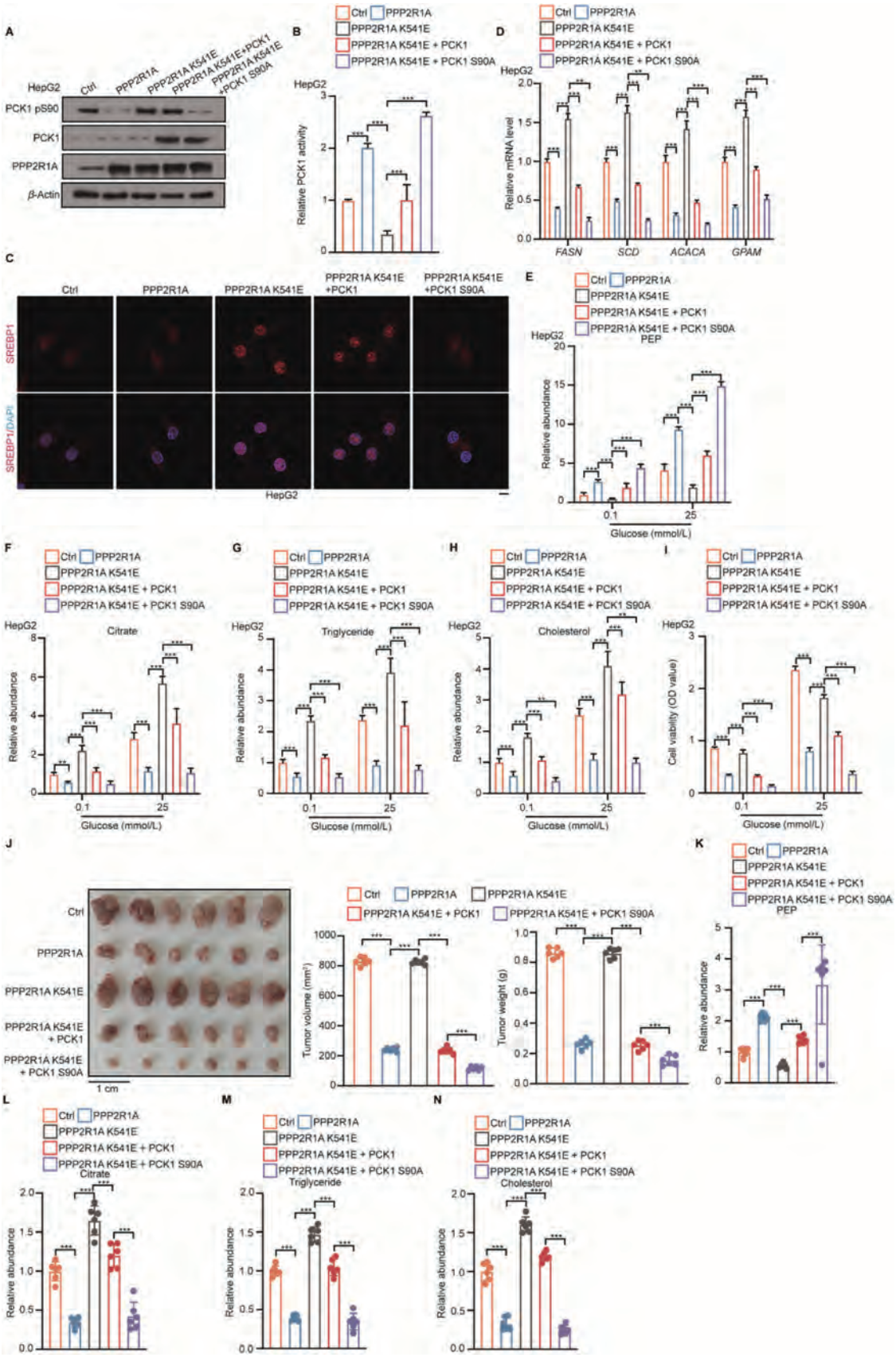

Figure 5 PPP2R1A promotes gluconeogenesis and inhibits lipogenesis by dephosphorylation of PCK1 Ser90 to suppress tumor growth. (A−I) HepG2 cells were transfected with plasmids overexpressing PPP2R1A or PPP2R1A mutant (K541E), or co-transfected with plasmids overexpressing PCK1 or PCK1 mutant (S90A), respectively. (A) The levels of PCK1 pS90, PCK1, PPP2R1A, and β-actin were tested by Western blot

were negatively correlated with the progression-free survival, and positively correlated with the TNM stage, but not the age and gender (Fig. S11C−S11F, Supporting Information Tables S6−S9). In addition, we report that HAT1 is a new succinyltransferase for the succinylation of phosphoglyceromutase 1 (PGAM1) to induce glycolysis in promoting tumor progression[23]. We observed that PGAM1 failed to affect the levels of PEP, citrate, triglyceride, and cholesterol in HepG2 cells (Supporting Information Fig. S12). Therefore, we conclude that HAT1 succinylates PPP2R1A K541, leading to phosphorylation of PCK1 Ser90 in liver cancer.

3.5. PPP2R1A promotes gluconeogenesis and inhibits lipogenesis by dephosphorylation of PCK1 Ser90 to suppress tumor growth

PPP2R1A, serving as a tumor suppressor, shows a high mutation rate in human cancers[29], but the role of PPP2R1A in liver cancer is still elusive. The effect of PPP2R1A on de-phosphorylation of PCK1 Ser90 is elusive. We supposed that PPP2R1A might inhibit the converting remodeling from gluconeogenesis to lipogenesis by de-phosphorylation of PCK1 Ser90. Interestingly, we observed that PPP2R1A, but not PPP2R1A (K541E), significantly repressed the levels of PCK1 pS90 in HepG2 and Huh7 cells, in which PCK1 (S90A) was able to reverse the effect of PPP2R1A (K541E) in the cells, suggesting that PPP2R1A confers the de-phosphorylation of PCK1 pS90 in a K541 succinylation-dependent manner (Fig. 5A and Supporting Information Fig. S13A). Intriguingly, the gluconeogenic enzyme activity of PCK1 was promoted by PPP2R1A, but was repressed by PPP2R1A (K541E) in HepG2 and Huh7 cells, and PCK1 or PCK1 (S90A) rescued PPP2R1A (K541E)-inhibited gluconeogenic enzyme activity of PCK1 in the cells (Fig. 5B and Fig. S13B). Conversely, PPP2R1A suppressed and PPP2R1A (K541E) enhanced nuclear accumulation of SREBP1 and expression of SREBP1 target genes associated with lipogenesis in HepG2 and Huh7 cells, while PCK1 or PCK1 (S90A) reversed the effect of PPP2R1A (K541E) on the phenotypes in the cells (Fig. 5C and D, Fig. S13C). Moreover, the PEP levels were increased and levels of citrate, triglyceride, cholesterol, and lipid accumulation were decreased by PPP2R1A. While, PPP2R1A (K541E) displayed an opposite effect on the phenotypes under both glucose-starved condition (0.1 mmol/L) and high glucose condition (25 mmol/L) in the HepG2 and Huh7 cells (Fig. 5E−H, Fig. S13D−S13H). Remarkably, PPP2R1A (K541E)-inhibited PEP levels were rescued and PPP2R1A (K541E)-induced levels of citrate, triglyceride, cholesterol, and lipid accumulation were reinforced by PCK1 or PCK1 (S90A) in the cells (Fig. 5E−H, Fig. S13D−S13H). The mutation of S90A reinforced the effect of PCK1 on the phenotypes in the system (Fig. 5B−H, Fig. S13B−S13H), suggesting that PPP2R1A restricts the remodeling of gluconeogenesis/lipogenesis by the de-phosphorylation of PCK1 Ser90.

Next, we investigated the effect of PPP2R1A-mediated de-phosphorylation of PCK1 Ser90 on liver cancer progression *in vitro* and *in vivo*. Interestingly, the cell viability was inhibited by PPP2R1A, while the mutation of K541E reversed the effect of PPP2R1A under both glucose-starved condition (0.1 mmol/L) and high glucose condition (25 mmol/L) in the HepG2 and Huh7 cells (Fig. 5I and Fig. S13I). Meanwhile, PCK1 or PCK1 (S90A) significantly blocked PPP2R1A (K541E)-induced cell viability in the system (Fig. 5I and Fig. S13I). Intriguingly, nude mice tumorigenicity experiments displayed that PPP2R1A repressed liver cancer growth and Ki-67 expression in the tumor tissues of the mice, while mutation of K541E restrained the effect of PPP2R1A on the phenotype (Fig. 5J and Fig. S13J). The over-expression of PPP2R1A could inhibit the levels of PCK1 pS90 in the tumor tissues from mice, but the PPP2R1A mutant (K541E) mimicking the HAT1-mediated succinylation promoted the levels of PCK1 pS90 in the system (Fig. S13K). However, PCK1 or PCK1 (S90A) blocked the effect of PPP2R1A (K541E) on PCK1 pS90 in the tumor tissues from mice. Importantly, we validated that PEP levels were enhanced, and levels of citrate, triglyceride, and cholesterol were reduced by PPP2R1A, and PPP2R1A (K541E) displayed an opposite effect on the metabolites in the tumor tissues from mice (Fig. 5K−N). In addition, PPP2R1A (K541E)-inhibited PEP levels were induced and PPP2R1A (K541E)-promoted levels of citrate, triglyceride, and cholesterol were suppressed by PCK1 or PCK1 (S90A) in the mice (Fig. 5K−N). Interestingly, we observed that the mutation of S90A reinforced the effect of PCK1 on the phenotypes in the system (Fig. 5I−N, Fig. S13I−S13K). Thus, we conclude that PPP2R1A promotes gluconeogenesis and inhibits lipogenesis by dephosphorylation of PCK1 Ser90 to suppress tumor growth.

3.6. Succinylation of PPP2R1A by HAT1 converses the role in modulation of remodeling of gluconeogenesis/lipogenesis to support liver cancer

Functionally, we further verified whether HAT1 promoted the tumor growth by triggering the converting remodeling from gluconeogenesis to lipogenesis involving PPP2R1A K541 succinylation/PCK1 pS90 signaling. HepG2 cell viability was significantly inhibited by HAT1 knockout, and re-expression of wild-type HAT1, but not HAT1 (T188A), could rescue the phenotype in

analysis in the cells. (B) The relative PCK1 activity was analyzed by the corresponding assay kit in the cells. (C) The nuclear accumulation of SREBP1 was observed by confocal immunofluorescence analysis in the cells. Scale bar, 5 μm. (D) The mRNA expression levels of SREBP1 target genes, including FASN, SCD, ACACA, and GPAM, were examined by RT-qPCR in the cells. (E−H) The relative levels of PEP, citrate, triglyceride, and cholesterol were analyzed by the corresponding assay kits in the cells cultured in 25 or 0.1 mmol/L glucose conditions for 10 h, respectively. (I) The cell viability was determined by CCK-8 assays cultured in 25 or 0.1 mmol/L glucose conditions for 10 h, respectively. (J−N) HepG2 cells were transfected with plasmids overexpressing PPP2R1A or PPP2R1A mutant (K541E), or co-transfected with plasmids over-expressing PCK1 or PCK1 mutant (S90A), respectively. The cells were subcutaneously injected into athymic nude mice ($n = 6$). (J) Representative images of tumors from the nude mice ($n = 6$) are shown. Tumor volumes and average tumor weight were calculated. Scale bar, 1 cm. (K−N) The relative levels of PEP, citrate, triglyceride, and cholesterol were analyzed by the corresponding assay kits in the tumor tissues from the nude mice. Data are presented as mean ± SD. Student's *t*-test, $^{**}P < 0.01$, $^{***}P < 0.001$. HAT1: histone acetyltransferase 1, PCK1: phosphoenolpyruvate carboxykinase 1, pS90: phosphorylation at serine 90, PPP2R1A: protein phosphatase 2 scaffold subunit alpha, SREBP1: sterol regulatory element-binding protein 1, FASN: fatty acid synthase, SCD: stearoyl-CoA desaturase, ACACA: acetyl-CoA carboxylase alpha, GPAM: glycerol-3-phosphate acyltransferase 1.

the cells (Fig. 6A and Supporting Information Fig. S14A). Interestingly, PCK1 or PCK1 (S90A), and PPP2R1A or PPP2R1A (K541R) could remarkably suppress the HAT1-induced proliferation of HepG2 cells, in which the mutation of S90A or K541R enhanced the effect of PCK1 or PPP2R1A on the suppression in the cells (Fig. 6A and Fig. S14A). Significantly, we observed that the depletion of HAT1 induced the apoptosis in HepG2 cells, while reconstitution of wild-type HAT1, but not HAT1 (T188A), restrained the apoptosis in the cells (Fig. S14B and S14C). In addition, PCK1/PCK1 (S90A) and PPP2R1A/PPP2R1A (K541R) rescued HAT1-inhibited apoptosis in the cells, in which the mutation of S90A or K541R enforced the function of PCK1 or PPP2R1A in the model (Fig. S14B and S14C).

Furthermore, nude mice tumorigenicity experiments showed that the depletion of HAT1 promoted the apoptosis in the tumor tissues, while reconstitution of wild-type HAT1, but not HAT1 (T188A), restrained the apoptosis in the model (Fig. S14D). PCK1/PCK1 (S90A) and PPP2R1A/PPP2R1A (K541R) rescued

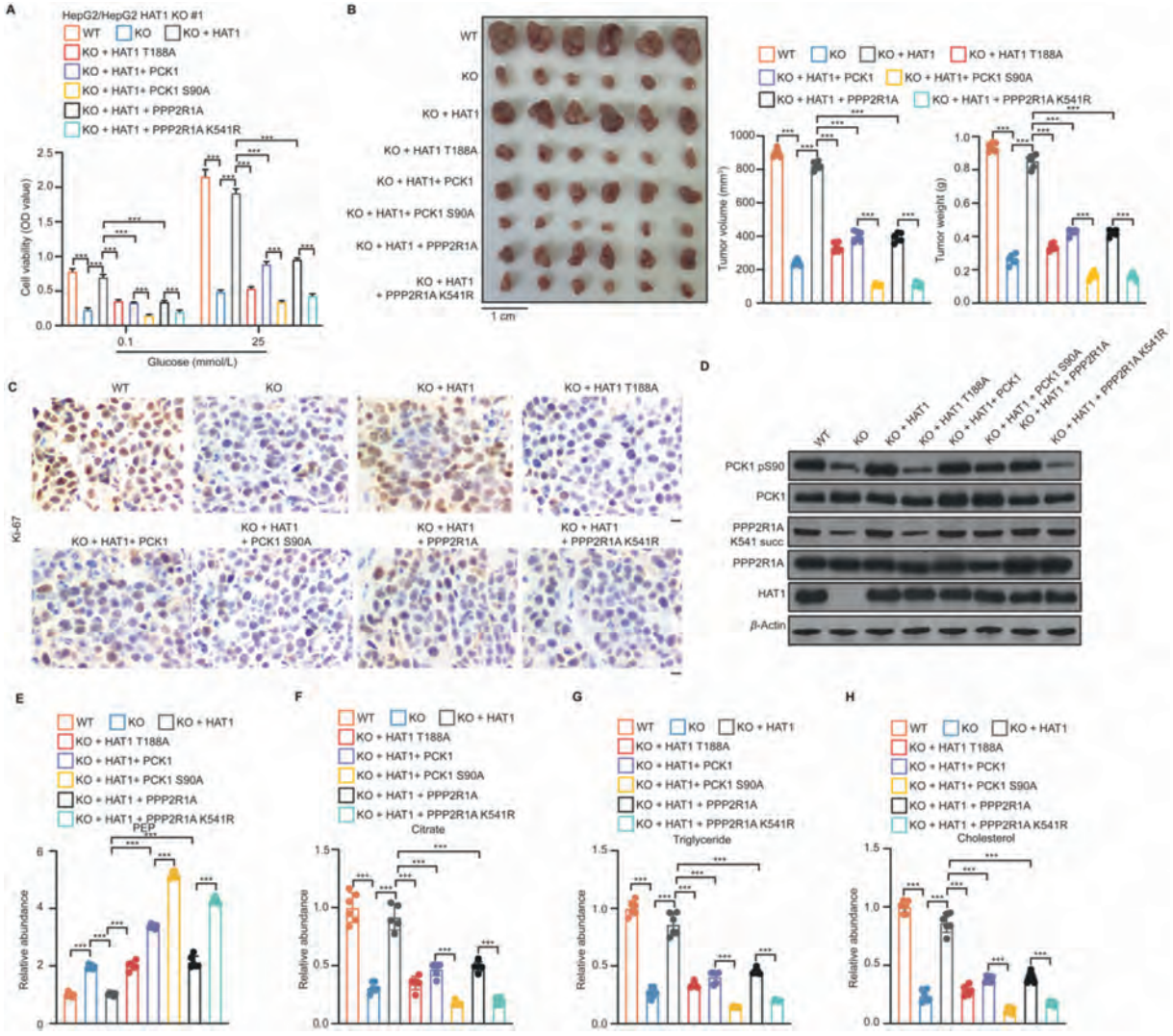

Figure 6 Succinylation of PPP2R1A by HAT1 converses the role in modulation of remodeling of gluconeogenesis/lipogenesis to support liver cancer. (A) The cell viability was analyzed by CCK-8 assays in HepG2 cells (WT), HAT1 KO #1 HepG2 cells, HAT1 KO #1 HepG2 cells reconstituted with wild-type HAT1 or HAT1 mutant (T188A), HAT1 KO #1 HepG2 cells co-reconstituted with wild-type HAT1 and PCK1, PCK1 mutant (S90A), PPP2R1A, or PPP2R1A mutant (K541R), respectively. (B−H) The athymic nude mice ($n = 6$) were subcutaneously injected with HepG2 cells (WT), HAT1 KO #1 HepG2 cells, HAT1 KO #1 HepG2 cells reconstituted with wild-type HAT1 or HAT1 mutant (T188A), HAT1 KO #1 HepG2 cells co-reconstituted with wild-type HAT1 and PCK1, PCK1 mutant (S90A), PPP2R1A, or PPP2R1A mutant (K541R), respectively. (B) Representative images of tumors from the nude mice ($n = 6$) were shown. Tumor volumes and average tumor weight were calculated. Scale bar = 1 cm. (C) The expression levels of Ki-67 were analyzed by IHC staining in the tumor tissues from the nude mice. Scale bar = 50 μm. (D) The levels of PCK1 pS90, PCK1, PPP2R1A, HAT1, and β-actin were examined by Western blot analysis in the tumor tissues from the nude mice. (E−H) The relative levels of PEP, citrate, triglyceride, and cholesterol were determined by the corresponding assay kits in the tumor tissues from the nude mice. Data are presented as mean ± SD. Student's t-test, $^{***}P < 0.001$. HAT1: histone acetyltransferase 1, PCK1: phosphoenolpyruvate carboxykinase 1, pS90: phosphorylation at serine 90, WT: wild type, KO: knockout, PPP2R1A: protein phosphatase 2 scaffold subunit alpha, IHC: immunohistochemistry, PEP: phosphoenolpyruvate.

HAT1-inhibited apoptosis, in which the mutation of S90A or K541R enforced the function of PCK1 or PPP2R1A in the model (Fig. S14D). The depletion of HAT1 repressed the growth of liver cancer and the levels of Ki-67 in the tumor tissues from mice, in which re-expression of wild-type HAT1, but not HAT1 (T188A), rescued the phenotypes in the mice (Fig. 6B and C, Fig. S14E). PCK1/PCK1 (S90A) and PPP2R1A/PPP2R1A (K541R) significantly reversed the roles of HAT1, in which mutation of S90A or K541R reinforced the impact in the model (Fig. 6B and C, Fig. S14E), suggesting that the succinylation of tumor suppressor PPP2R1A displays an oncogene function. Meanwhile, we also validated that HAT1 promoted PCK1 pS90 through modulation of PPP2R1A succinylation in the mouse model. We observed that the levels of PCK1 pS90 were inhibited by HAT1 knockout. The reconstitution of HAT1 could reverse the phenotype in the tumor tissues from mice, but HAT1 (T188A) failed to work (Fig. 6D). Importantly, PPP2R1A/PPP2R1A (K541R) was able to converse the effect of HAT1 on the metabolites, in which the mutation of K541R presented a more significant impact in the mice (Fig. 6D). Remarkably, IHC staining shown that HAT1 knockout could reduce the levels of PCK1 pS90, nuclear SREBP1, and PPP2R1A K541 succinylation in the tumor tissues from mice. The reconstitution of HAT1 could reverse the phenotype in the tumor tissues from mice, but HAT1 (T188A) failed to work (Supporting Information Fig. S15A−S15D). PCK1/PCK1 (S90A) and PPP2R1A/PPP2R1A (K541R) significantly reversed the effect of HAT1 on PCK1 pS90, nuclear SREBP1, and PPP2R1A K541 succinylation, but the mutation of S90A or K541R reinforced more impact in the model (Fig. S15A−S15D). Meanwhile, we further evaluated the roles of HAT1 in remodeling from gluconeogenesis to lipogenesis by PPP2R1A K541 succinylation and PCK1 phosphorylation in the mouse model. Consistently, PEP levels were increased, and levels of citrate, triglyceride, and cholesterol were decreased by HAT1 knockout and reconstitution of HAT1, but not HAT1 (T188A), could reverse the phenotype in the tumor tissues from mice (Fig. 6E−H). Importantly, PCK1/PCK1 (S90A) and PPP2R1A/PPP2R1A (K541R) were able to converse the effect of HAT1 on the metabolites, in which mutation of S90A or K541R displayed a more significant impact in the mice (Fig. 6E−H). Taken together, we conclude that succinylation of PPP2R1A by HAT1 converses the role in modulation of remodeling of gluconeogenesis/lipogenesis to support liver cancer.

4. Discussion

Cancer cells display key oncogene-driven remodeling of metabolic signaling to meet the endless metabolic demands[39]. Gluconeogenesis is inhibited and lipogenesis is induced in cancer cells[9,40], but the underlying mechanism of remodeling of gluconeogenesis/lipogenesis in tumors is poorly understood. Our group reports that HAT1 is a new succinyltransferase in promoting tumor progression[23]. PPP2R1A is required for the assembly of the phosphatase PP2A holoenzymes and shows a high mutation rate in cancers. However, the key divers modulating the remodeling of gluconeogenesis/lipogenesis in tumors is still unclear. In this study, we investigated the underlying mechanism by which HAT1 modulates the remodeling of gluconeogenesis/lipogenesis in tumors.

It has been reported that the coordination of multiple PTMs plays a pivotal role in metabolic remodeling in tumorigenesis[15,41]. Acetyltransferase HAT1 demonstrates a variety of PTM functions[20] and our group reports HAT1 succinylates PGAM1 to induce glycolysis in promoting tumor progression[23,42]. HAT1 promotes cancer immune escape by upregulating expression of programmed death-ligand 1 in pancreatic cancer[43]. HAT1 contributes to gemcitabine resistance of pancreatic cancer by targeting the PVT1/EZH2 complex[44]. Strikingly, using DEN/CCl_4-induced liver cancer mouse model we surprisingly observed that the liver cancer incidence was reduced in the liver-specific Hat1 knockout mice relative to controls. It strongly suggests that HAT1 is essential for DEN/CCl_4-induced hepatocarcinogenesis.

To elucidate the biological function of HAT1 in hepatocarcinogenesis, a multi-omics, including RNA-sequencing, phosphoproteomics, and untargeted metabolomics, was performed. KEGG pathway analysis of differentially expressed genes, different phosphoproteins and metabolites displayed the crucial effect of HAT1 on several crucial signaling pathways, such as Hippo signaling pathway, AMPK signaling pathway, and glycolysis/gluconeogenesis signaling pathway. It suggests that HAT1 may globally affect the cellular physiological and pathological processes at different levels. Our finding implies that HAT1 may contribute to the hepatocarcinogenesis by affecting gluconeogenesis and lipogenesis signaling. Thus, in this study, we focused on the significance of gluconeogenesis or lipogenesis affected by HAT1 depletion in the liver at both physiological conditions and DEN/CCl_4-induced liver cancer model.

The gluconeogenesis is inhibited, and glycolysis is activated in cancer cells to produce sufficient energy for the endless proliferation[8,45]. As a rate-limiting enzyme in gluconeogenesis, PCK1 has been well-recognized as a critical tumor suppressor in cancer progression[46]. PCK1 inhibits CHK2 *O*-GlcNAcylation during hepatocellular carcinoma cell growth[47]. PCK1 suppresses the liver cancer progression through TCA cataplerosis, oxidative stress, and cancer cell apoptosis by regulating metabolic remodeling[11]. A recent study reports that AKT-mediated phosphorylation of PCK1 at serine 90 activates SREBP proteins and the transcription of downstream lipogenesis-related genes, inducing lipogenesis and liver cancer development[13]. Based on these findings, in our study, we supposed that HAT1 might modulate PCK1 pS90 in the remodeling of gluconeogenesis/lipogenesis in tumors. We observed that the levels of HAT1 and PCK1 pS90 were elevated, but PCK1 expression was reduced in the liver cancer tissues from DEN/CCl_4-induced mice relative to controls and in the liver cancer cell lines relative to PHH, while the knockout of HAT1 significantly repressed the phenotype. Clinically, IHC staining analysis supported that the expression of HAT1 was positively correlated with the PCK1 pS90 levels in the tissues of liver cancer. Moreover, we observed that the depletion of HAT1 repressed the PCK1 pS90 levels in these cancer cell lines, such as liver cancer, cholangiocarcinoma, pancreatic cancer, and renal cancer, but not in those cancer cell lines including breast cancer, esophageal squamous cell carcinoma, colon cancer, gastric cancer, lung cancer, and cervical cancer Hela. It implies that HAT1 may globally affect PCK1-mediated remodeling of gluconeogenesis/lipogenesis in some cancers. Interestingly, our data showed that the gluconeogenic enzyme activity of PCK1 was inhibited by HAT1 in liver cancer cells, PCK1 (S90D) was remarkably repressed and PCK1 (S90A) induced HAT1-inhibited gluconeogenic enzyme activity in the cells. It suggests that HAT1 confers the PCK1-mediated remodeling of gluconeogenesis/lipogenesis in liver cancer. Other phosphorylation sites on PCK1 that affect the remodeling of gluconeogenesis/lipogenesis will be further investigated in the future. It has been reported that AKT interacts with PCK1 and

induces phosphorylation of PCK1 pS90[13]. In this study, we observed that the exogenous S90A potentially suppressed endogenous PCK1 pS90 levels in the cells. HAT1 failed to affect the expression and phosphorylation of AKT in HepG2 cells. It suggests that the exogenous PCK1 S90A mutant may competitively bind to AKT and suppress the endogenous PCK1 pS90 levels in cells.

Then, we try to identify the mechanism by which HAT1 promotes the remodeling of gluconeogenesis/lipogenesis. Lysine succinylation is a critical mechanism for the regulation of metabolism in cancers. It has been reported that SIRT5-mediated SDHA desuccinylation contributes to progression of clear cell renal cell carcinoma by targeting metabolic pathways[48]. PRMT5 promotes lipid metabolism remodeling by SIRT7-mediated desuccinylation during tumor growth and metastasis[49]. Considering that HAT1 succinylated PGAM1 to promote glycolysis of cancer cells[23], we demonstrated that HAT1 catalyzed PPP2R1A succinylation to limit the interaction among PCK1, PPP2R1A, and PPP2CA, followed by the dephosphorylation of PCK1 Ser90 in the remodeling of gluconeogenesis/lipogenesis. In our study, the succinylation of PPP2R1A K541 could be detectable in the cells, mouse model, and patient tissues using the antibody against succinylation of PPP2R1A K541 (PPP2R1A K541 succ) and the *in vitro* succinylation assays. Moreover, LC−MS/MS and chemical labeling-based detection methods can be used to better understand the significance of succinylation of PPP2R1A K541 in cancers. Meanwhile, the mutation of PPP2R1A K541 or PCK1 S90 using CRISPR Cas9 knock-in in the human liver cell lines will be performed in future studies. Our finding provides a new insight into the mechanism by which HAT1-mediated succinylation of PPP2R1A K541 modulates remodeling of gluconeogenesis/lipogenesis in tumors.

It has been reported that PP2A is a tumor suppressor by the regulation of dephosphorylation in cancer cells[26,50]. Chk1 reactivates the activity of PP2A tumor suppressor in tumor cells[51]. Suppression of STRN3-containing PP2A reverses the activity of Hippo tumor suppressor in gastric cancer[52]. However, the function of PP2A and PPP2R1A in liver cancer is poorly understood. Interestingly, we found that PPP2R1A inhibited the converting remodeling of gluconeogenesis/lipogenesis by dephosphorylation of PCK1 Ser90, which suppressed the tumor growth. The coordinated regulation and crosstalk of different PTMs play a critical role in cancer progression[15,16]. Theretofore, we conclude that PPP2R1A suppresses the tumor growth by repressing the remodeling of gluconeogenesis/lipogenesis. However, succinylation of PPP2R1A lysine 541 by HAT1 converses the role in modulation of remodeling of gluconeogenesis/lipogenesis to support liver cancer. Thus, the succinylation of tumor suppressor PPP2R1A displays an oncogene function. Up to now, PTMs converting tumor suppressor function to oncogene have not been reported. Our finding provides new insights into the mechanism by which PTMs confer the conversion of tumor suppressor function to oncogene.

Overall, we summarize a model for our study (Fig. 7). In this model, PPP2R1A is required for the assembly of PP2A

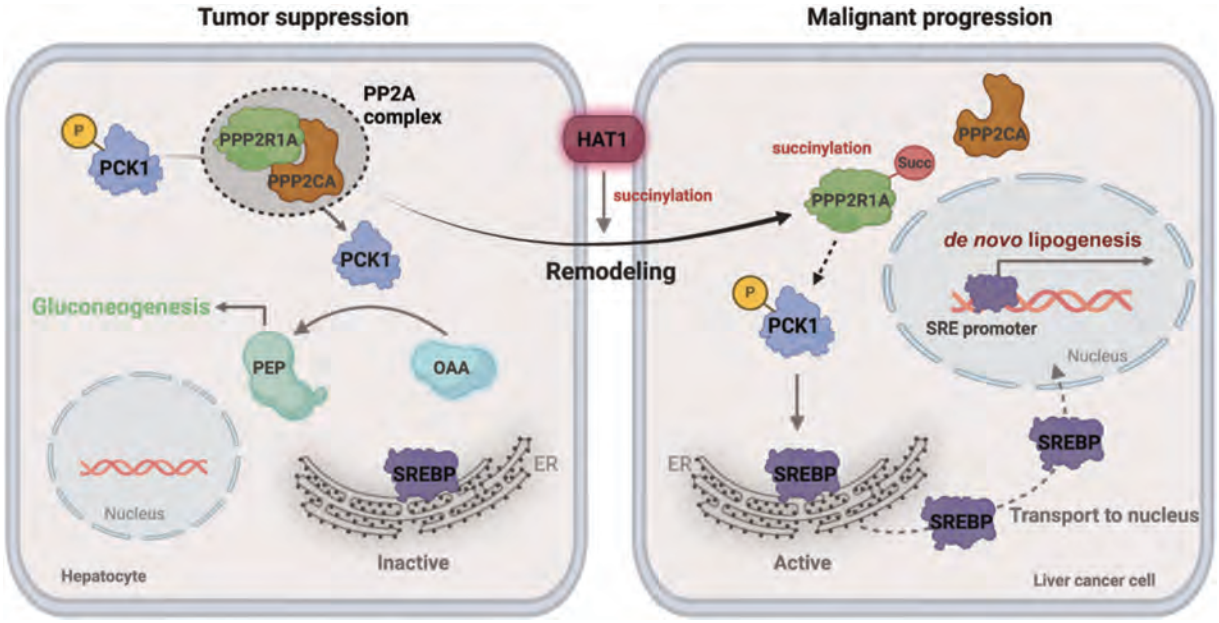

Figure 7 Succinylation of PPP2R1A lysine 541 by HAT1 converses the role in modulation of remodeling of gluconeogenesis/lipogenesis to support liver cancer. In this model, PP2A is a protein complex that contains 60 different holoenzymes, PPP2R1A and PPP2CA are representative members of A and C subunits of PP2A in hepatocytes. PPP2R1A is required for the assembly of the PP2A complex. PCK1 catalyzes the conversion of OAA to PEP in gluconeogenesis. PPP2R1A promotes gluconeogenesis and inhibits lipogenesis by de-phosphorylation of PCK1 Ser90, leading to the tumor suppression of liver cancer. HAT1 contributes to the remodeling of gluconeogenesis/lipogenesis in liver cancer. PPP2R1A is succinylated at K541 by HAT1, leading to the inhibition of assembly of PP2A in liver cancer. Inhibition of assembly of PP2A blocks the dephosphorylation of PCK1 Ser90, which induces lipogenesis but fails to catalyze the conversion of OAA to PEP in gluconeogenesis, contributing to the malignant progression of liver cancer. Thus, the succinylation of tumor suppressor PPP2R1A displays an oncogene function. HAT1: histone acetyltransferase 1, PCK1: phosphoenolpyruvate carboxykinase 1, PPP2R1A: protein phosphatase 2 scaffold subunit alpha, PPP2CA: protein phosphatase 2 catalytic subunit alpha, PP2A: protein phosphatase 2A, OAA: oxaloacetate, PEP: phosphoenolpyruvate, SREBP1: sterol regulatory element-binding protein 1.

holoenzyme, resulting in the inhibition of remodeling of gluconeogenesis/lipogenesis by PCK1 S90 dephosphorylation, leading to the depression of tumor growth. PPP2R1A K541 is succinylated by HAT1 to block the interaction among PCK1, PPP2R1A, and PPP2CA, followed by the inhibition of assembly of PP2A holoenzyme, restraining the dephosphorylation of PCK1 S90. Functionally, PPP2R1A suppresses the tumor growth by repressing the remodeling of gluconeogenesis/lipogenesis, while succinylation of PPP2R1A lysine 541 by HAT1 converses the role in modulation of remodeling of gluconeogenesis/lipogenesis to support liver cancer. Therefore, the succinylation of tumor suppressor PPP2R1A displays an oncogene function.

Acknowledgments

This work was supported by the National Natural Science Foundation of China (Nos. 82103066, 82372818, 82303210, and 82302887) and Tianjin Key Medical Discipline (Specialty) Construction Project (TJYXZDXK-009A, China).

Author contributions

Guang Yang: Writing − original draft, Investigation, Funding acquisition, Data curation, Conceptualization. Yufei Wang: Validation, Methodology, Investigation, Funding acquisition. Hongfeng Yuan: Validation, Investigation, Funding acquisition. Huihui Zhang: Validation, Investigation. Lina Zhao: Validation, Investigation. Chunyu Hou: Validation, Investigation. Pan Lv: Validation, Investigation. Jihui Hao: Conceptualization, Writing − review & editing, Supervision, Project administration. Xiaodong Zhang: Writing − review & editing, Supervision, Project administration, Funding acquisition, Conceptualization.

Conflicts of interest

The authors declare no conflicts of interest.

Data availability

The datasets (and computer code) produced in this study are available in the following databases: (1) The mass spectrometry proteomics (phosphoproteomics) data have been deposited to the ProteomeXchange Consortium (http://proteomecentral.proteomexchange.org) *via* the iProX partner repository with the dataset identifier PXD043633. (2) RNA−seq data have been deposited to the SRA database with the dataset identifier PRJNA992217 (Temporary Submission ID: SUB13606163).

Appendix A. Supporting information

Supporting information to this article can be found online at https://doi.org/10.1016/j.apsb.2025.07.040.

References

1. Martinez-Reyes I, Chandel NS. Cancer metabolism: looking forward. *Nat Rev Cancer* 2021;**21**:669−80.
2. Calderaro J, Ziol M, Paradis V, Zucman-Rossi J. Molecular and histological correlations in liver cancer. *J Hepatol* 2019;**71**:616−30.
3. Li X, Ramadori P, Pfister D, Seehawer M, Zender L, Heikenwalder M. The immunological and metabolic landscape in primary and metastatic liver cancer. *Nat Rev Cancer* 2021;**21**:541−57.
4. Wang C, Cao Y, Yang C, Bernards R, Qin W. Exploring liver cancer biology through functional genetic screens. *Nat Rev Gastroenterol Hepatol* 2021;**18**:690−704.
5. Jin T, Wang C, Tian Y, Dai C, Zhu Y, Xu F. Mitochondrial metabolic reprogramming: an important player in liver cancer progression. *Cancer Lett* 2020;**470**:197−203.
6. Du D, Liu C, Qin M, Zhang X, Xi T, Yuan S, et al. Metabolic dysregulation and emerging therapeutical targets for hepatocellular carcinoma. *Acta Pharm Sin B* 2022;**12**:558−80.
7. Vander Heiden MG, DeBerardinis RJ. Understanding the intersections between metabolism and cancer biology. *Cell* 2017;**168**:657−69.
8. Grasmann G, Smolle E, Olschewski H, Leithner K. Gluconeogenesis in cancer cells - repurposing of a starvation-induced metabolic pathway? *Biochim Biophys Acta Rev Cancer* 2019;**1872**:24−36.
9. Bian X, Jiang H, Meng Y, Li YP, Fang J, Lu Z. Regulation of gene expression by glycolytic and gluconeogenic enzymes. *Trends Cell Biol* 2022;**32**:786−99.
10. Bechmann LP, Hannivoort RA, Gerken G, Hotamisligil GS, Trauner M, Canbay A. The interaction of hepatic lipid and glucose metabolism in liver diseases. *J Hepatol* 2012;**56**:952−64.
11. Liu MX, Jin L, Sun SJ, Liu P, Feng X, Cheng ZL, et al. Metabolic reprogramming by PCK1 promotes TCA cataplerosis, oxidative stress and apoptosis in liver cancer cells and suppresses hepatocellular carcinoma. *Oncogene* 2018;**37**:1637−53.
12. Shao W, Espenshade PJ. Expanding roles for SREBP in metabolism. *Cell Metab* 2012;**16**:414−9.
13. Xu D, Wang Z, Xia Y, Shao F, Xia W, Wei Y, et al. The gluconeogenic enzyme PCK1 phosphorylates INSIG1/2 for lipogenesis. *Nature* 2020;**580**:530−5.
14. Jiang H, Zhu L, Xu D, Lu Z. A newly discovered role of metabolic enzyme PCK1 as a protein kinase to promote cancer lipogenesis. *Cancer Commun (Lond)* 2020;**40**:389−94.
15. Pan S, Chen R. Pathological implication of protein post-translational modifications in cancer. *Mol Aspect Med* 2022;**86**:101097.
16. Chen L, Liu S, Tao Y. Regulating tumor suppressor genes: post-translational modifications. *Signal Transduct Targeted Ther* 2020;**5**:90.
17. Sabari BR, Zhang D, Allis CD, Zhao Y. Metabolic regulation of gene expression through histone acylations. *Nat Rev Mol Cell Biol* 2017;**18**:90−101.
18. Sun L, Zhang H, Gao P. Metabolic reprogramming and epigenetic modifications on the path to cancer. *Protein Cell* 2022;**13**:877−919.
19. Gruber JJ, Geller B, Lipchik AM, Chen J, Salahudeen AA, Ram AN, et al. HAT1 coordinates histone production and acetylation via H4 promoter binding. *Mol Cell* 2019;**75**:711−724 e5.
20. Zhang X, Hou C, Yang G. Highlighted multi-modifications of enzymes: a novel succinylation mediated by histone acetyltransferase 1 in tumors. *Cancer Biol Med* 2021;**19**:133−5.
21. Zhu Z, Han Z, Halabelian L, Yang X, Ding J, Zhang N, et al. Identification of lysine isobutyrylation as a new histone modification mark. *Nucleic Acids Res* 2021;**49**:177−89.
22. Delaney K, Tan M, Zhu Z, Gao J, Dai L, Kim S, et al. Histone lysine methacrylation is a dynamic post-translational modification regulated by HAT1 and SIRT2. *Cell Discov* 2021;**7**:122.
23. Yang G, Yuan Y, Yuan H, Wang J, Yun H, Geng Y, et al. Histone acetyltransferase 1 is a succinyltransferase for histones and non-histones and promotes tumorigenesis. *EMBO Rep* 2021;**22**:e50967.
24. Kou F, Wu L, Zheng Y, Yi Y, Ji Z, Huang Z, et al. HMGB1/SET/HAT1 complex-mediated SASH1 repression drives glycolysis and metastasis in lung adenocarcinoma. *Oncogene* 2023;**42**:3407−21.
25. Vainonen JP, Momeny M, Westermarck J. Druggable cancer phosphatases. *Sci Transl Med* 2021;**13**.
26. Ronk H, Rosenblum JS, Kung T, Zhuang Z. Targeting PP2A for cancer therapeutic modulation. *Cancer Biol Med* 2022;**19**:1428−39.

27. Seshacharyulu P, Pandey P, Datta K, Batra SK. Phosphatase: PP2A structural importance, regulation and its aberrant expression in cancer. *Cancer Lett* 2013;**335**:9−18.
28. Lenaerts L, Reynhout S, Verbinnen I, Laumonnier F, Toutain A, Bonnet-Brilhault F, et al. The broad phenotypic spectrum of PPP2R1A-related neurodevelopmental disorders correlates with the degree of biochemical dysfunction. *Genet Med* 2021;**23**:352−62.
29. Haesen D, Abbasi Asbagh L, Derua R, Hubert A, Schrauwen S, Hoorne Y, et al. Recurrent PPP2R1A mutations in uterine cancer act through a dominant-negative mechanism to promote malignant cell growth. *Cancer Res* 2016;**76**:5719−31.
30. Zhou L, Zhang S, Wang L, Liu X, Yang X, Qiu L, et al. PCYT2 inhibits epithelial-mesenchymal transition in colorectal cancer by elevating YAP1 phosphorylation. *JCI Insight* 2024;**9**:e178823.
31. Kang Q, Ma D, Zhao P, Chai X, Huang Y, Gao R, et al. BRG1 promotes progression of B-cell acute lymphoblastic leukemia by disrupting PPP2R1A transcription. *Cell Death Dis* 2024;**15**:621.
32. Lee HW, Kyung T, Yoo J, Kim T, Chung C, Ryu JY, et al. Real-time single-molecule co-immunoprecipitation analyses reveal cancer-specific Ras signalling dynamics. *Nat Commun* 2013;**4**:1505.
33. Gao Y, Feng J, Yang G, Zhang S, Liu Y, Bu Y, et al. Hepatitis B virus X protein-elevated MSL2 modulates hepatitis B virus covalently closed circular DNA by inducing degradation of APOBEC3B to enhance hepatocarcinogenesis. *Hepatology* 2017;**66**:1413−29.
34. Wang Y, Guo YR, Liu K, Yin Z, Liu R, Xia Y, et al. KAT2A coupled with the alpha-KGDH complex acts as a histone H3 succinyltransferase. *Nature* 2017;**552**:273−7.
35. Zhang T, Zhang J, You X, Liu Q, Du Y, Gao Y, et al. Hepatitis B virus X protein modulates oncogene Yes-associated protein by CREB to promote growth of hepatoma cells. *Hepatology* 2012;**56**:2051−9.
36. Tu ML, Liu HX, Zhang R, Chen H, Mao FJ, Cheng SZ, et al. Analysis and evaluation of the inhibitory mechanism of a novel Angiotensin-I-Converting enzyme inhibitory peptide derived from casein hydrolysate. *J Agric Food Chem* 2018;**66**:4139−44.
37. Fu Y, Alashi AM, Young JF, Therkildsen M, Aluko RE. Enzyme inhibition kinetics and molecular interactions of patatin peptides with angiotensin I-converting enzyme and renin. *Int J Biol Macromol* 2017; **101**:207−13.
38. Zhao L, Yuan H, Wang Y, Geng Y, Yun H, Zheng W, et al. HBV confers innate immune evasion through triggering HAT1/acetylation of H4K5/H4K12/miR-181a-5p or KPNA2/cGAS-STING/IFN-I signaling. *J Med Virol* 2023;**95**:e28966.
39. Pan C, Li B, Simon MC. Moonlighting functions of metabolic enzymes and metabolites in cancer. *Mol Cell* 2021;**81**:3760−74.
40. Cheng C, Geng F, Cheng X, Guo D. Lipid metabolism reprogramming and its potential targets in cancer. *Cancer Commun (Lond)* 2018;**38**:27.
41. Zhu Y, Lin X, Zhou X, Prochownik EV, Wang F, Li Y. Post-translational control of lipogenesis in the tumor microenvironment. *J Hematol Oncol* 2022;**15**:120.
42. Wang YF, Zhao LN, Geng Y, Yuan HF, Hou CY, Zhang HH, et al. Aspirin modulates succinylation of PGAM1K99 to restrict the glycolysis through NF-kappaB/HAT1/PGAM1 signaling in liver cancer. *Acta Pharmacol Sin* 2023;**44**:211−20.
43. Fan P, Zhao J, Meng Z, Wu H, Wang B, Wu H, et al. Overexpressed histone acetyltransferase 1 regulates cancer immunity by increasing programmed death-ligand 1 expression in pancreatic cancer. *J Exp Clin Cancer Res* 2019;**38**:47.
44. Sun Y, Ren D, Zhou Y, Shen J, Wu H, Jin X. Histone acetyltransferase 1 promotes gemcitabine resistance by regulating the PVT1/EZH2 complex in pancreatic cancer. *Cell Death Dis* 2021;**12**:878.
45. Feng J, Li J, Wu L, Yu Q, Ji J, Wu J, et al. Emerging roles and the regulation of aerobic glycolysis in hepatocellular carcinoma. *J Exp Clin Cancer Res* 2020;**39**:126.
46. Wang Z, Dong C. Gluconeogenesis in cancer: function and regulation of PEPCK, FBPase, and G6Pase. *Trends Cancer* 2019;**5**: 30−45.
47. Xiang J, Chen C, Liu R, Gou D, Chang L, Deng H, et al. Gluconeogenic enzyme PCK1 deficiency promotes CHK2 O-GlcNAcylation and hepatocellular carcinoma growth upon glucose deprivation. *J Clin Investig* 2021;**131**:e144703.
48. Ma Y, Qi Y, Wang L, Zheng Z, Zhang Y, Zheng J. SIRT5-mediated SDHA desuccinylation promotes clear cell renal cell carcinoma tumorigenesis. *Free Radic Biol Med* 2019;**134**:458−67.
49. Yuan HF, Zhao M, Zhao LN, Yun HL, Yang G, Geng Y, et al. PRMT5 confers lipid metabolism reprogramming, tumour growth and metastasis depending on the SIRT7-mediated desuccinylation of PRMT5 K387 in tumours. *Acta Pharmacol Sin* 2022;**43**:2373−85.
50. Vervoort SJ, Welsh SA, Devlin JR, Barbieri E, Knight DA, Offley S, et al. The PP2A-Integrator-CDK9 axis fine-tunes transcription and can be targeted therapeutically in cancer. *Cell* 2021;**184**. 3143-62.e32.
51. Khanna A, Kauko O, Bockelman C, Laine A, Schreck I, Partanen JI, et al. Chk1 targeting reactivates PP2A tumor suppressor activity in cancer cells. *Cancer Res* 2013;**73**:6757−69.
52. Tang Y, Fang G, Guo F, Zhang H, Chen X, An L, et al. Selective inhibition of STRN3-Containing PP2A phosphatase restores Hippo tumor-suppressor activity in gastric cancer. *Cancer Cell* 2020;**38**. 115-28.e9.